Hamiltonian averaging and integrability in nonlinear systems with periodically varying dispersion

S. B. Medvedev and S. K. Turitsyn
Institute of Computational Technologies, Siberian Branch of the Russian Academy of Sciences, 630090 Novosibirsk, Russia;
Institute of Automation and Electrometry, Siberian Branch of the Russian Academy of Sciences, 630090 Novosibirsk, Russia

(Submitted 4 March 1999)
Pis'ma Zh. Éksp. Teor. Fiz. **69**, No. 7, 465–470 (10 April 1999)

By applying Hamiltonian averaging and a quasi-identity-like transformation it is demonstrated that the averaged dynamics of high-frequency nonlinear waves in systems with periodically varying dispersion can be described in a particular limit by the integrable nonlinear Schrödinger equation. © *1999 American Institute of Physics.* [S0021-3640(99)00107-3]

PACS numbers: 05.45.Yv, 42.65. Tg, 42.81.Dp

Propagation of high-frequency large-amplitude waves in media with varying dispersion is a rather general nonlinear problem with a wide area of physical applications, such as, for instance, optical pulse transmission in dispersion-managed fiber lines,[1] stretched pulse generation in mode-locking fiber laser systems,[2] propagation of high-intensity beams in second-order nonlinear media with periodic poling, soliton evolution in a periodically modulated nonlinear waveguide, and other applications. Optical pulse transmission in fibers is one of the brightest demonstrations of practical application of the fundamental soliton theory. The traditional path-averaged optical soliton preserves its cosh-type shape during propagation by compensating on average the fiber dispersion through nonlinearity. This is possible because the pulse power oscillations (due to periodic amplification of the pulse to compensate for the fiber loss) are very fast. Rapid oscillations of the power can be averaged out, and, as a result, the slow pulse dynamics in the traditional soliton-based transmission lines is governed by the integrable[3] nonlinear Schrödinger equation (NLSE). Interability of the NLSE makes it possible to apply the well-developed and powerful mathematical method of the inverse-scattering transform[3] to a variety of practical problems (see, e.g., Refs. 4–7 and references therein). Experimental (and even the first commercial[8]) implementations of multichannel soliton transmission have stimulated further research in soliton theory. In this paper we apply Hamiltonian averaging and quasi-identity transformation to demonstrate that the averaged dynamics of high-frequency nonlinear waves in systems with periodically varying dispersion can be described in some particular limits by the integrable NLSE. As a specific physical and practical application, in the present paper we focus on dispersion-managed soliton transmission. The dispersion-managed (DM) periodic, breathing, soliton-like pulse that stably propagates in a fiber system with large variations of the dispersion

differs substantially from the fundamental (NLSE) soliton.[9–29] There are two scales in the DM pulse propagation: the first (fast dynamics) corresponds to rapid oscillations of the pulse width and power due to periodic variations of the dispersion and periodic amplification; and the second (slow dynamics) occurs due to the combined effects of nonlinearity, residual dispersion, and averaged effects. The traditional soliton solution of the NLSE with uniform dispersion and without loss realizes a continuous balance between nonlinearity and dispersion. Losses and variations of dispersion make it impossible in the general case to support such a balance continuously. Nevertheless, a balance between nonlinear effects and dispersion can be achieved *on average* over the compensation period. As a result, the slow dynamics of the DM soliton can be described by the propagation equation averaged over fast oscillations.[1,12] The DM pulse dynamics typically depends on many system parameters and is rather complicated. Different theoretical approaches have been developed to describe the properties of the DM soliton: the variational approach[12–20] or the more advanced root-mean-square momentum method,[1,21] multiscale analysis[22–24] methods using averaging,[12,26,1,29,25] including averaging in the spectral domain,[12,13] and expansion of the DM soliton in a basis of chirped Gauss–Hermite functions.[27,28,1]

Because of the practical importance of this problem, it is of obvious interest to develop different theoretical methods to describe the main properties of the basic model in different limits. A variety of complementary mathematical methods can be advantageously used to find an optimal and economical description of any specific practical application. In this paper, using Hamiltonian averaging and quasi-identity-like transform,[30] we demonstrate that in some specific limits (including , in particular, a weak dispersion map[26]) the DM soliton is described by the integrable NLSE.

The evolution (in z) of a high-frequency wave in medium with periodically varying dispersion and nonlinearity is governed by the NLSE with periodic coefficients $d(z)$ and $c(z)$ (we assume here that both have the same period), which can be written in the Hamiltonian form

$$i\frac{\partial A}{\partial z}=\{A,H\}=\frac{\delta H}{\delta A^*}=-d(z)A_{tt}-\epsilon\, c(z)|A|^2A, \tag{1}$$

with the Hamiltonian

$$H=\int\left\{d(z)\left|A_t\right|^2-\varepsilon\frac{c(z)}{2}\left|A\right|^4\right\}dt \tag{2}$$

and the Poisson brackets defined as

$$\{F,G\}=\int\left(\frac{\delta F}{\delta A(t,z)}\,\frac{\delta G}{\delta A^*(t,z)}-\frac{\delta F}{\delta A^*(t,z)}\,\frac{\delta G}{\delta A(t,z)}\right)dt. \tag{3}$$

In Eq. (1) the distance z is normalized by the compensation period L, $d(z)=\tilde{d}+\langle d\rangle$ ($\langle\tilde{d}\rangle=0$) describes the varying dispersion, and $c(z)$ corresponds to power oscillations (due to loss and amplification). For notation we refer to our previous papers.[1,27,13] The small parameter $\epsilon=L/Z_{NL}$, where L is a compensation period and Z_{NL} (see, e.g., Refs. 13,1) is a characteristic nonlinear scale. The true DM soliton is a solution of Eq. (1) of the form $A(z,t)=\exp(ikz)\,M(z,t)$ with a periodic function $M(z+L,t)=M(z,t)$. The DM

soliton can be viewed as a kind of nonlinear Bloch wave in the language of solid-state physics. The goal of the theoretical analysis is to present a systematic way to describe family of solutions M with different k. The basic idea suggested in Refs. 1 and 12 is to use a small parameter ϵ to derive a path-averaged model that gives a systematic, leading-order description of the DM soliton. Averaging cannot be performed directly in Eq. (1) because of the large variations of $\tilde{d} \gg \langle d \rangle$. However, path-averaged propagation equation can be obtained in the frequency domain.[12,13] The approach developed in Ref. 12 can be considered as a decomposition of DM pulse dynamics in the fast evolution of the phase and a slow evolution of the amplitude. The shape of the DM soliton then is given by nonlocal nonlinear equation, steady state solutions of which give the leading-order approximation of DM solitons. In this paper we show that in some limits an averaged equation can be transformed to the *integrable* NLSE. First, following Refs. 12 and 13, we do the Fourier transform

$$A(t,z) = \int A_\omega \exp[-i\omega t]\, d\omega \quad (\text{here } A_\omega = A(\omega,z))$$

and rewrite the basic equation in the frequency domain.

Equation (1) then takes the form

$$i\frac{\partial A_\omega}{\partial z} - d(z)\,\omega^2 A_\omega + \epsilon \int F_{\omega 123}(z)\,\delta(\omega+\omega_1-\omega_2-\omega_3)\,A_1^* A_2 A_3 d\omega_1 d\omega_2 d\omega_3 = 0, \qquad (4)$$

where $F_{\omega 123} = c(z)$. To eliminate the periodic dependence of the linear part we (following Refs. 12,13) apply the so-called Floquet–Lyapunov transformation[30]

$$A_\omega = \phi_\omega \exp\{-i\,\omega^2 R_0(z) - i\,\theta(\omega)\}, \quad dR_0/dz = d(z) - \langle d \rangle. \qquad (5)$$

We have included here the phase factor $\theta(\omega)$, which does not change the z dependence of the coefficients. The aim of this transformation is to eliminate the large coefficient $\tilde{d}$ from (1). In the new variables the equation has the form

$$i\frac{\partial \phi_\omega}{\partial z} - \langle d \rangle\,\omega^2\,\phi_\omega + \epsilon \int G_{\omega 123}(z)\,\delta(\omega+\omega_1-\omega_2-\omega_3)\,\phi_1^*\,\phi_2\,\phi_3\,d\omega_1 d\omega_2 d\omega_3 = 0; \qquad (6)$$

here $G_{\omega 123}(z) = c(z)\exp\{i\Delta\Omega R_0(z) + i\Delta\theta\}$ and $\Delta\Omega = \omega^2 + \omega_1^2 - \omega_2^2 - \omega_3^2$, $\Delta\theta = \theta_\omega + \theta_1 - \theta_2 - \theta_3$. Note that $G_{\omega 123}$ depends only on the specific combination of the frequencies given by the resonance surface $\Delta\Omega$. Both the Fourier and the Floquet–Lyapunov transform (5) are canonical, and the transformed Hamiltonian H is

$$H = \langle d \rangle \int \omega^2 |\phi_\omega|^2 d\omega - \varepsilon \int \frac{G_{\omega 123}}{2}\,\delta(\omega+\omega_1-\omega_2-\omega_3)\,\phi_\omega^*\phi_1^*\phi_2\phi_3 d\omega d\omega_1 d\omega_2 d\omega_3. \qquad (7)$$

Now we apply Hamiltonian averaging. Let us make the following change of the variables

$$\phi_\omega = \varphi_\omega + \epsilon \int V_{\omega 123}\,\delta(\omega+\omega_1-\omega_2-\omega_3)\,\varphi_1^*\,\varphi_2\,\varphi_3\,d\omega_1 d\omega_2 d\omega_3,$$

$$V_{\omega 123}(z) = i\int_0^z [G_{\omega 123}(\tau) - T_{\omega 123}]\,d\tau,$$

with

$$T_{\omega 123}=\langle G_{\omega 123}\rangle=\int_0^1 G_{\omega 123}(z)dz=\int_0^1 c(z)\ \exp\{i\Delta\Omega R_0(z)+i\Delta\theta\}dz. \tag{8}$$

The path-averaged equation has the form

$$i\frac{\partial\varphi_\omega}{\partial z}-\langle d\rangle\,\omega^2\,\varphi_\omega+\epsilon\int T_{\omega 123}\,\delta(\omega+\omega_1-\omega_2-\omega_3)\,\varphi_1^*\,\varphi_2\,\varphi_3\,d\omega_1 d\omega_2 d\omega_3=0. \tag{9}$$

Here $\varphi(\omega)$ is assumed to decay sufficiently fast to ensure convergence of the integral. This equation was first derived in Refs. 12, 13 using simple physical considerations. Since the ϕ_ω vary slowly, in the leading approximation, on the scale of one period, we can neglect their evolution and integrate Eq. (6) over the period, placing ϕ_ω outside of the integrals over z. The Hamiltonian averaging introduced here presents a regular way to calculate next-order corrections to the averaged model. From the Hamiltonian structure of the starting equation it is clear that the matrix element $T_{\omega 123}$ has the following symmetries (compare with Ref. 31)

$$T_{\omega 123}=T_{1\omega 23}=T_{\omega 132}=T^*_{23\omega 1}. \tag{10}$$

In the case of the lossless model ($c(z)=c_0=$const; for details see Ref. 1) and a two-step dispersion map built from a piece of a fiber with dispersion $d_1+\langle d\rangle$ and length l_1 followed by a piece of fiber with dispersion $d_2+\langle d\rangle$ and length $l_2=1-l_1$ ($d_1l_1+d_2(1-l_1)=0$), the matrix element $T_{\omega 123}$ takes the especially simple form

$$T_{\omega 123}=c_0\,\frac{\sin[\mu\Delta\Omega/2]}{\mu\Delta\Omega/2}. \tag{11}$$

The parameter $\mu=d_1l_1$ introduced here is a characteristic of the map strength. Strong dispersion management corresponds to large $\mu\gg\langle d\rangle$ and the so-called weak map corresponds to $\mu\ll\langle d\rangle$. We demonstrate below that, in particular, in the limit of small μ the averaged equation (9) can be transformed to the NLSE. Note that Eq. (9) possesses a remarkable property: The matrix element $T_{\omega 123}=\Phi(\Delta\Omega)\exp\{i\Delta\theta\}$ is a function of $\Delta\Omega$, and

$$\Phi(0)=\int_0^1 c(z)dz=\langle c\rangle,\quad \Phi'(0)=i\langle c\,R_0\rangle=i\int_0^1 c(z)\,R_0(z)dz \tag{12}$$

on the resonant surface

$$\omega+\omega_1-\omega_2-\omega_3=0,\quad \Delta\Omega=\omega^2+\omega_1^2-\omega_2^2-\omega_3^2=0. \tag{13}$$

This observation allows us to make the following quasi-identity-like transformation, which eliminates the variable part of the matrix element $T_{\omega 123}$

$$\varphi_\omega=a_\omega+\frac{\epsilon}{\langle d\rangle}\int\frac{T_{\omega 123}-T_0}{\Delta\Omega}a_1^*\,a_2\,a_3\,\delta(\omega+\omega_1-\omega_2-\omega_3)\,d\omega_1 d\omega_2 d\omega_3, \tag{14}$$

where $T_0=\Phi(0)\exp\{i\Delta\theta\}$. This transformation has no singularities. If the integral part in this transform is small compared with a_ω, then in the leading order we get for a_ω

$$i\frac{\partial a_\omega}{\partial z}-\langle d\rangle\,\omega^2\,a_\omega+\epsilon\int T_0\,\delta(\omega+\omega_1-\omega_2-\omega_3)\,a_1^*\,a_2\,a_3\,d\omega_1 d\omega_2 d\omega_3=0. \tag{15}$$

This is nothing more than the integrable nonlinear Schrödinger equation written in the frequency domain (here we choose $\theta=0$).

Obviously, this is a quasi-identity transformation only if the integral in Eq. (14) is small compared with a_ω. This is not so in the general case, and that is why the typical DM soliton has a form different from the cosh-like shape usual for the NLSE soliton. However, if the kernel function in Eq. (14) is small,

$$|S(\Delta\Omega)|=\left|\frac{T_0-T_{\omega 123}(\Delta\Omega)}{\Delta\Omega}\right|\ll 1, \tag{16}$$

then the averaged model can be reduced to the NLSE. In other terms, this is a condition on the functions $c(z)$ and $d(z)$ under which a quasi-identity transformation is possible. For instance, one can check that for the two-step map described above, in the limit $\mu\to 0$ this transformation is, indeed, a quasi-identity transformation and the path-averaged model is the NLSE. Thus, we can express (in this limit) solutions of equation (9), and, consequently, of the original equation (1) via solutions of the NLSE in the explicit form:

$$A(t,z)=\int a_\omega\,e^{\{-i\omega t-i\omega^2 R_0-i\theta\}}d\omega+\epsilon\int W_{\omega 123}\,a_1^*\,a_2\,a_3\,\delta(\omega+\omega_1-\omega_2-\omega_3)$$
$$\times d\omega_1 d\omega_2 d\omega_3 d\omega,$$

where

$$W_{\omega 123}(z)=\left(V_{\omega 123}+\frac{T_{\omega 123}-T_0}{\langle d\rangle\,\Delta\Omega}\right)\,\exp\{-i\omega t-i\omega^2 R_0(z)-i\theta(\omega)\} \tag{17}$$

and a_ω is a solution of the NLSE (15).

The averaging transformation can also be presented as

$$\phi_\omega=\varphi_\omega+\varepsilon\frac{\delta K}{\delta\varphi_\omega}=\varphi_\omega-\varepsilon\{K,\varphi_\omega\}. \tag{18}$$

Therefore, this transform can be viewed as the leading-order term in the expansion of a canonical exponential (Lie) transformation

$$\phi_\omega=\exp[\{\varepsilon K,\dots\}]\varphi_\omega, \tag{19}$$

with the functional

$$K=\int\frac{V_{\omega 123}}{2}\delta(\omega+\omega_1-\omega_2-\omega_3)\varphi_\omega^*\varphi_1^*\varphi_2\varphi_3 d\omega d\omega_1 d\omega_2 d\omega_3.$$

After averaging the Hamiltonian H takes the form

$$\langle H\rangle=\langle d\rangle\int\omega^2|\varphi_\omega|^2 d\omega-\varepsilon\int\frac{T_{\omega 123}}{2}\delta(\omega+\omega_1-\omega_2-\omega_3)$$
$$\times\varphi_\omega^*\varphi_1^*\varphi_2\varphi_3 d\omega d\omega_1 d\omega_2 d\omega_3. \tag{20}$$

The quasi-identity transform of the Hamiltonian $\langle H\rangle$ ($T_{\omega 123}\rightarrow T_0$) is given by Eq. (19) with a corresponding functional K_1:

$$K_1=\int \frac{T_{\omega 123}-T_0}{2\langle d\rangle \Delta\Omega}\,\delta(\omega+\omega_1-\omega_2-\omega_3)a_\omega^* a_1^* a_2 a_3 d\omega d\omega_1 d\omega_2 d\omega_3 .$$

In conclusion, using Hamiltonian averaging and quasi-identity-like transformation, we have shown that in some specific limits nonlinear wave propagation in a system with periodically varying dispersion and nonlinearity can be described by the integrable NLSE.

[1] S. K. Turitsyn, E. G. Shapiro, and V. K. Mezentsev, Opt. Fiber Technol.: Mater., Devices Syst. **4**, 384 (1998).
[2] H. A. Haus, K. Tamura, L. E. Nelson, and E. P. Ippen, IEEE J. Quantum Electron. **31**, 591 (1995).
[3] V. E. Zakharov and A. B. Shabat, Zh. Éksp. Teor. Fiz. **60**, 136 (1971); Sov. Phys. JETP **33**, 77 (1971).
[4] E. A. Kuznetsov, A. M. Rubenchik, and V. E. Zakharov, Phys. Rep. **142**, 103 (1986).
[5] M. J. Ablowitz and P. A. Clarkson, *Solitons, Nonlinear Evolution Equations, and Inverse Scattering*, Cambridge University Press, Cambridge, UK, 1991.
[6] A. C. Newell and J. V. Moloney, *Nonlinear Optics*, Addison-Wesley Publishing Company, Redwood City CA, 1992.
[7] E. A. Kuznetsov, A. V. Mikhailov, and I. A. Shimokhin, Physica D **87**, 201 (1995).
[8] N. Robinson *et al.*, ''4xSONET OC-192 Field Installed Dispersion Managed Soliton System over 450 km of Standard Fiber in the 1550 nm Erbium Band,'' Post Deadline presentation, PD19-1, OFC'98, San Jose, USA.
[9] N. Smith, F. M. Knox, N. J. Doran *et al.*, Electron. Lett. **32**, 55 (1995).
[10] J. H. B. Nijhof, N. J. Doran, W. Forysiak, and F. M. Knox, Electron. Lett. **33**, 1726 (1997).
[11] M. Wald, I. M. Uzunov, F. Lederer, and S. Wabnitz, Photon. Techn. Lett. **9**, 1670 (1997).
[12] I. Gabitov and S. K. Turitsyn, Opt. Lett. **21**, 327 (1996); JETP Lett. **63**, 861 (1996).
[13] I. Gabitov, E. G. Shapiro, and S. K. Turitsyn, Opt. Commun. **134**, 317 (1996); Phys. Rev. E **55**, 3624 (1997).
[14] M. Matsumoto and H. A. Haus, IEEE Photonics Technol. Lett. **9**, 785 (1997).
[15] N. Kutz, P. Holmes, S. Evangelides, and J. Gordon, J. Opt. Soc. Am. B **15**, 87 (1997).
[16] V. S. Grigoryan, T. Yu, E. A. Golovchenko *et al.*, Opt. Lett. **22**, 1609 (1997).
[17] T. Georges, J. Opt. Soc. Am. B **15**, 1553 (1998).
[18] T. Lakoba, J. Yang, D. J. Kaup, and B. A. Malomed, Opt. Commun. **149**, 366 (1998).
[19] E. G. Shapiro and S. K. Turitsyn, Phys. Rev. E **56**, (1997); Opt. Fiber Technol.: Mater., Devices Syst. **4**, 151 (1998).
[20] S. K. Turitsyn, I. Gabitov, E. W. Laedke *et al.*, Opt. Commun. **151**, 117 (1998).
[21] S. K. Turitsyn, T. Schaefer, and V. K. Mezentsev, Phys. Rev. E **58**, R5264 (1998).
[22] T.-S. Yang and W. L. Kath, Opt. Lett. **22**, 985 (1997).
[23] T. S. Yang, W. L. Kath, and S. K. Turitsyn, Opt. Lett. **23**, 985 (1998).
[24] M. J. Ablowitz and G. Biondini, Opt. Lett. **23**, 1123 (1998).
[25] S. K. Turitsyn and V. K. Mezentsev, JETP Lett. **68**, 830 (1998).
[26] A. Hasegawa, Y. Kodama, and A. Maruta, Opt. Fiber Technol.: Mater., Devices Syst. **3**, 197 (1997).
[27] S. K. Turitsyn and V. K. Mezentsev, JETP Lett. **67**, 640 (1998); S. K. Turitsyn, T. Schaefer, and V. K. Mezentsev, Opt. Lett. **23**, 1351 (1998).
[28] T. Lakoba and D. J. Kaup, Electron. Lett. **34**, 1124 (1998).
[29] S. K. Turitsyn, A. B. Aceves, C. K. R. T. Jones, and V. Zharnitsky, Phys. Rev. E **58**, 48 (1998).
[30] V. I. Arnold, *Geometrical Methods in the Theory of Ordinary Differential Equations*, New York, Springer-Verlag, 1988.
[31] V. E. Zakharov, V. S. L'vov, and G. Falkovich, *Kolmogorov Spectra of Turbulence*, Springer-Verlag, Berlin, 1992.

Published in English in the original Russian journal. Edited by Steve Torstveit.

The static $Q\bar{Q}$ interaction at small distances and OPE violating terms

Yu. A. Simonov
Institute of Theoretical and Experimental Physics

(Submitted 4 February 1999; resubmitted 16 February 1999)
Pis'ma Zh. Éksp. Teor. Fiz. **69**, No. 7, 471–473 (10 April 1999)

The nonperturbative contribution to the one-gluon exchange produces a universal linear term in the static potential at small distances $\Delta V = 6N_c\alpha_s\sigma r/2\pi$. Its role in the resolution of long-standing discrepancies in the fine splitting of heavy quarkonia and improving agreement with lattice data for static potentials is examined, and implications for operator product expansion (OPE) violating terms in other processes are discussed. © *1999 American Institute of Physics.*
[S0021-3640(99)00207-8]

PACS numbers: 12.38.Bx, 12.38.Gc, 14.70.Dj

1. Possible nonperturbative contributions from small distances have drawn a lot of attention recently.[1,2] In terms of the interquark potential the appearance of linear terms in the static potential $V(r)=\text{const}\,r$, where r is the distance between charges, implies violation of OPE, since const $\sim$ (mass)^2, and this dimension is not available in terms of field operators. There is however some analytical[1,2] and numerical[3] evidence for the possible existence of such terms $O(m^2/Q^2)$ in the asymptotic expansion at large Q.

On a more phenomenological side the presence of a linear term at small distances $r<T_g$, where T_g is the gluonic correlation length,[4,5] is required by at least two sets of data.

First, the detailed lattice data[6] do not support the much weaker quadratic behavior of $V(r)\sim\text{const}\cdot r^2$ that follows from the OPE and the field correlator method[4,5] but instead favor the same linear form $V(r)=\sigma r$ at all distances (in addition to the perturbative $-C_2\alpha_s/r$ term). Second, a small-distance linear term is necessary for the description of the fine splitting in heavy quarkonia, since the spin–orbit Thomas term $V_t = -(1/2m^2r)(dV/dr)$ is sensitive to the small-r region, and an additional linear contribution at $r<T_g$ is needed to fit the experimental splitting.[7] Moreover, lattice calculations[8] exhibit $1/r$ behavior of V_t in all of the measured region up to $r=0.1$ fm.

Of crucial importance is the sign of the $O(m^2/Q^2)$ term, since the usual screening correction (real m) leads to a negative sign of the linear potential, and one needs small-distance nonperturbative (NP) dynamics, which produces a negative (tachyonic) sign of m^2 (Refs. 1,2). Phenomenological implications of such contributions have been studied in detail in Ref. 1. In what follows we show that the interaction of the gluon spin with the NP background indeed yields a tachyonic gluon mass at small distances.

2. In this letter we report the first application of the systematic background perturbation theory[9,10] to the problem in question. One starts with the decomposition of the full gluon vector potential A_μ into the NP background B_μ and perturbative field a_μ,

$$A_\mu = B_\mu + a_\mu, \tag{1}$$

and make use of the 'tHooft identity for the partition function

$$Z = \int DA_\mu e^{-S(A)} = \frac{1}{N}\int DB_\mu \eta(B) \int Da_\mu e^{-S(B+a)}, \tag{2}$$

where $\eta(B)$ is the weight for NP fields, defining the vacuum averages, e.g.,

$$g^2\langle F^B_{\mu\nu}(x)\Phi^B(x,y)F^B_{\lambda\sigma}(y)\rangle_B = \frac{\hat{1}}{N_c}(\delta_{\mu\lambda}\delta_{\nu\sigma} - \delta_{\mu\sigma}\delta_{\nu\lambda})D(x-y) + \Delta_1, \tag{3}$$

where $F^B_{\mu\nu}$ and Φ^B are the field strength and parallel transporter made of B_μ only; Δ_1 is the full derivative term[4] not contributing to the string tension σ, which is

$$\sigma = \frac{1}{2N_c}\int d^2x D(x) + O(\langle FFFF\rangle). \tag{4}$$

The background perturbation theory is an expansion of the last integral in (2) in powers of ga_μ and an averaging over B_μ with the weight $\eta(B_\mu)$, as shown in (3). Referring the reader to Refs. 9 and 10 for explicit formalism and renormalization, we concentrate below on the static interquark interaction at small r. To this end we consider the Wilson loop of size $r\times T$, where T is large, $T\to\infty$, and define

$$\langle W\rangle_{B,a} = \left\langle P\exp\left[ig\int_C (B_\mu + a_\mu)dz_\mu\right]\right\rangle_{B,a} \equiv \exp\{-V(r)T\}. \tag{5}$$

Expanding (5) in powers of ga_μ, we obtain

$$\langle W\rangle = W_0 + W_2 + \ldots; \quad V = V_0(r) + V_2(r) + V_4(r) + \ldots, \tag{6}$$

where $V_n(r)$ corresponds to $(ga_\mu)^n$ and can be expressed in terms of D, Δ_1, and higher correlators.[5,9]

Coming now to $V_2(r)$, describing one exchange of a perturbative gluon in the background, we find from the term quadratic in a_μ in $S(B+a)$ in the background Feynman gauge the gluon Green's function

$$G_{\mu\nu} = -(D^2_\lambda\delta_{\mu\nu} + 2igF^B_{\mu\nu})^{-1}, \quad D^{ca}_\lambda = \partial_\lambda\delta_{ca} + gf^{cba}B^b_\lambda. \tag{7}$$

Expanding in powers of $gF^B_{\mu\nu}$, we can write $G_{\mu\nu}$ as

$$G = -D^{-2} + D^{-2}2igF^BD^{-2} - D^{-2}2igF^BD^{-2}2igF^BD^{-2} + \ldots, \tag{8}$$

and the first term on the right-hand side of (8) corresponds to the spinless gluon exchange, propagating in the confining film covering the Wilson loop.[9,10] As was shown recently,[11] the term D^{-2} produces only weak corrections $O(r^3)$ to the usual perturbative potential at small distances, while it corresponds to the massive spinless propagator with mass m_0 at large distances.

In what follows we concentrate on the third term in (8), which yield

$$W_2^{(3)} = T\int \frac{\alpha_s(k^2)}{\pi^2}\,\frac{d^3k e^{i\mathbf{kr}}\mu^2(k^2)}{(\mathbf{k}^2+m_0^2)^2} = -\Delta V_2(r)T, \tag{9}$$

where we have defined, having in mind Eq. (4),

$$\mu^2(k^2) = 6\int \frac{D(z)e^{-ikz}d^4z}{4\pi^2 z^2}; \qquad \mu^2(0) = \frac{6\sigma N_c}{2\pi}. \tag{10}$$

From Eq. (10) we obtain the following positive contribution to the potential $V_2(r)$ at small r (we neglect a constant term $O(1/m_0)$:

$$\Delta V_2(r) = \mu^2(k_{\text{eff}})\alpha_s(k_{\text{eff}})r + O(r^2), \quad r \lesssim T_g. \tag{11}$$

Analysis of the integral (9) shows that $k_{\text{eff}} \sim 1/r$, and therefore $\Delta V_2(r)$ is determined mostly by the short-distance dynamics.

3. The analysis done heretofore concerns the static interquark potential and reveals that even at small distances the NP background provides some contribution which is incorporated in the negative mass-squared term $-\mu^2$.

Applying the same NP background formalism to other processes of interest, one would get similar corrections of the order of μ^2/p^2, as was investigated in Ref. 1.

To check the self-consistency of our results, one can find the contribution of $\mu^2(k)$ to the correlator D,

$$D(q) \sim \alpha_s(q)\int \frac{d^4p\,\mu^2(p)}{(p^2+m_0^2(p))^2(q-p)^2} \sim \frac{1}{q^2}, \quad q^2 \to \infty, \tag{12}$$

which is positive and consistent with recent lattice data.[3] Insertion of (12) into (10) yields constant $\mu^2(p)$ at large p (modulo logarithms), which implies self-consistent NP dynamics at small distances (large p). It is worthwhile to note also that the negative sign of the μ^2 contribution is directly connected to the asymptotic freedom, where the same paramagnetic term in the effective action S_{eff} (Ref. 12) enters with the negative sign, and one can take into account that $-\mu^2(x,y) \sim \delta^2 S_{\text{eff}}/\delta a_\mu(x)\delta a_\mu(y)$.

The author is grateful for discussions, correspondence and very useful remarks to V. I. Zakharov and helpful discussions to V. A. Novikov and V. I. Shevchenko.

The financial support of RFFI through Grants 97-02-16404 and 97-0217491 is gratefully acknowledged.

[1] K. G. Chetyrkin, S. Narison, and V. I. Zakharov, http://xxx.lanl.gov/abs/hep-ph/9811275.
[2] R. Akhoury and V. I. Zakharov, Phys. Lett. B **438**, 165 (1998); F. J. Yndurain, http://xxx.lanl.gov/abs/hep-ph/9708448, Nucl. Phys. B (Proc. Suppl.) **64**, 433 (1998).
[3] G. Burgio, F. Di Renzo, G. Marchesini, and E. Onofri, Phys. Lett. B **422**, 219 (1998).
[4] H. G. Dosch and Yu. A. Simonov, Phys. Lett. B **205**, 339 (1988); for a review see Yu. A. Simonov, Phys. Usp. **39**, 313 (1996); hep-ph/9709344.
[5] Yu. A. Simonov, Nucl. Phys. B **324**, 67 (1989).
[6] S. P. Booth, D. S. Henry, A. Hulsebos *et al.*, Phys. Lett. B **234**, 385 (1992); G. Bali, K. Schilling, and A. Wachter, http://xxx.lanl.gov/abs/hep-lat/9506017.
[7] A. M. Badalian and V. P. Yurov, Yad. Fiz. **56**, 239 (1993); A. M. Badalian and Yu. A. Simonov, Yad. Fiz. **59**, 2247 (1996).
[8] K. D. Born, E. Laermann, R. Sommer *et al.*, Phys. Lett. B **329**, 332 (1994); G. S. Bali, K. Schilling, and A. Wachter, Phys. Rev. D **56**, 2566 (1997).

[9] Yu. A. Simonov, JETP Lett. **57**, 525 (1993); Yad. Fiz. **58**, 113 (1995).
[10] Yu. A. Simonov, in *Lecture Notes in Physics*, Vol. 479, Springer-Verlag, Berlin, 1996.
[11] Yu. A. Simonov, http://xxx.lanl.gov/abs/hep-ph/9902233.
[12] A. M. Polyakov, *Gauge Fields and Strings*, Harwood Acad. Publ., Chur, Switzerland, 1987, Ch. 2.

Published in English in the original Russian journal. Edited by Steve Torstveit.

Universality in effective strings

S. Jaimungal, G. W. Semenoff, and K. Zarembo
Department of Physics and Astronomy, University of British Columbia, 6224 Agricultural Road, Vancouver, British Columbia V6T 1Z1, Canada

(Submitted 9 March 1999)
Pis'ma Zh. Éksp. Teor. Fiz. **69**, No. 7, 474–480 (10 April 1999)

It is demonstrated that, due to the finite thickness of domain walls and the consequent ambiguity in defining their locations, the effective string description obtained by integrating out bulk degrees of freedom contains ambiguities in the coefficients of the various geometric terms. The only term with unambiguous coefficient is the zeroth-order Nambu–Goto term. We argue that fermionic ghost fields which implement gauge-fixing act to balance these ambiguities. The renormalized string tension, obtained after integrating out both bulk and world sheet degrees of freedom, can be defined in a scheme-independent manner; explicit finite expressions are computed, to one-loop, for the case of compact quantum electrodynamics and φ^4 theory. © *1999 American Institute of Physics.* [S0021-3640(99)00307-2]

PACS numbers: 11.25.Db, 12.20.Ds

A long-standing problem in the physics of interfaces in three-dimensional systems is to describe the interface dynamics as a theory of fluctuating surfaces analogous to an effective Euclidean string theory.[1–3] The interface surface can be interpreted as the world sheet of an effective string in three dimensions, while the two phases on either side of the interface represent the vacuum expectation values of a fundamental field. For example, in the Ising model the field is the spin operator, and the interface is the set of links about which the spin changes sign. An effective string action of this surface has a typical geometric expansion which begins with the Nambu–Goto term (the area), next the extrinsic curvature, and then higher-order curvature corrections. It is usually argued that the higher-order corrections are irrelevant as far as the low energy dynamics is concerned, and perturbation theory consisting in keeping only the area term and extrinsic curvature is valid. However, we will demonstrate that such an ansatz is in fact ambiguous from the outset. In particular, we will demonstrate that coefficients of the higher-order curvatures are completely arbitrary, and depend upon the precise prescription implemented in defining the position of the interface. Such an ambiguity is a direct consequence of the finite thickness of the interface region. In spite of this ambiguity an effective string description is possible if one includes in the action fermionic degrees of freedom which reinstate the scheme-independent nature of the fundamental action.

In this work we concentrate on interfaces which occur in 3D compact quantum electrodynamics (QED).[4] The analysis can be easily applied to any other field theory in 3D which has a soliton solution to the classical equations of motion. In compact QED,

monopole instantons cause the electric fields between two charged particles to form a flux tube, the potential between electric charges grows linearly with the distance between them, and the charges are confined.[4] This picture of confinement is, however, a purely classical one. In the full quantum theory the string of electric flux, along with the magnetic fields in the bulk, are not rigid but rather fluctuate.

Compact QED can be regarded as the low-energy effective theory for the Georgi–Glashow model, where the $SU(2)$ symmetry is spontaneously broken to $U(1)$. The monopoles appearing in the broken gauge theory are the classical solutions of the original Higgs model which have finite Euclidean action.[5] The collection of monopoles behave as a gas of charged particles interacting through a Coulomb force. Since the charges are of order $\sqrt{4\pi}/g$, where g is the gauge coupling, the monopole configurations can be treated using a semiclassical approximation in the limit of weak gauge coupling. The system then reduces to the classical thermodynamics of a Coulomb gas and the partition function is a sine-Gordon (SG) theory:[4]

$$Z=\int [d\varphi]\exp\left\{-\frac{g^2}{32\pi^2}\int d^3x\,[(\partial\varphi)^2-2m^2{:}\cos\varphi{:}]\right\}. \tag{1}$$

The monopole density is the coefficient of the cosine interaction, $\zeta=g^2m^2/32\pi^2$. The grand canonical partition function for the monopoles is recovered by expanding in powers of ζ and performing the functional integral over φ. In the presence of the monopole solution the photon becomes massive and Wilson loop correlators obey an area law.[4] The relevant order parameter in the original gauge theory (compact QED) is the vacuum expectation value of the Wilson loop. There is a natural mapping between this correlator and the following correlation function in the SG model:[4,6]

$$W(C)\equiv\left\langle \exp\left(\frac{i}{2}\oint_C dA\right)\right\rangle_{\rm QED}=\left\langle \exp\left(\frac{g^2}{16\pi}\int_S \star d\varphi\right)\right\rangle_{\rm SG}. \tag{2}$$

Here S is an arbitrary surface bounded by the contour C. The result can be shown to be independent of the choice of this surface. We are interested in the behavior of (2) for large loops. The contour C will be assumed to lie at infinity in the $x_3=0$ plane. In this case, it is possible to reformulate the problem. The operator on the right hand side of (2) introduces a source for the SG field or, equivalently, one may assume that φ experiences a jump of magnitude 2π across the surface S. Since the potential is periodic in φ, this jump can be eliminated by shifting φ on one side of the surface by 2π. This shift renders the field continuous; however, it changes the boundary conditions as $x_3\to+\infty$. Consequently, performing such a shift on φ reduces (2) to an evaluation of the path integral (1) with the boundary conditions $\varphi\to 0$ as $x_3\to-\infty$ and $\varphi\to 2\pi$ as $x_3\to+\infty$. These boundary conditions are precisely what is required for field configurations in the presence of a domain wall. The domain wall in this case describes a world sheet of a string of electric flux created by charges at infinity.

The first step in obtaining an effective string action is to obtain the classical solution satisfying the appropriate boundary conditions. The solution is the SG soliton:

$$\varphi_{\rm cl}(x)=4\arctan\, e^{mx_3}, \tag{3}$$

which corresponds to a domain wall in the $x_3=0$ plane. The position of this domain wall is in fact ambiguous. Conventionally, its position is given by the surface on which $\varphi=\pi$.[6,7] However, other definitions are also possible, for example, the surface on which the energy density is maximal.[8,9] These definitions, although agreeing at the classical level, do not agree once quantum corrections are included. Nevertheless, they will yield the same result within an order of m^{-1}. This uncertainty is due to the finite thickness of the domain wall and we will argue that this ambiguity translates into the nonuniversality of the world-sheet action.

Upon inserting (3) as a classical background field in the functional integral over φ in (1), the collective coordinate method can be used to separate the integral over fluctuations into an integral over the domain wall position, which we describe by a height function $f(x_1,x_2)$, and over the field fluctuations in the bulk:

$$Z=\int [d\varphi][df]\Delta_{\mathrm{FP}}[\varphi]\delta[K[f,\phi]]\, e^{-S_{\mathrm{SG}}[\varphi]}, \tag{4}$$

where $K[f,\phi]=\int dx_3 K(\mathbf{x},x_3-f)\varphi(x)-\pi$ and $\Delta_{\mathrm{FP}}[\varphi]=\delta K[f,\phi]/\delta f$ is the Faddeev–Popov determinant, $\mathbf{x}$ is (x_1,x_2), and S_{SG} is the same as in (1). A particular definition of the domain wall position corresponds to choosing a kernel K. There is no unique choice of this function. The definition of Refs. 6 and 7 corresponds to $K=\delta(x_3-f)$, while the standard collective coordinate method,[8,9] in which the fluctuations of the domain wall are associated with quasi-zero modes in the background of the classical solution (3), corresponds to $K=\varphi'_{\mathrm{cl}}(x_3-f)$.

Integrating over φ in (4) yields an effective action for the coordinate $f(\mathbf{x})$ of the domain wall. In the semiclassical approximation φ is replaced by its classical solution. The effective action is then given by

$$S_{\mathrm{eff}}=\sigma_0\int\left(1+\frac{1}{2}(\boldsymbol{\nabla}f)^2\right)+\mathcal{O}((\boldsymbol{\nabla}f)^2), \tag{5}$$

where the string tension is determined by the mass of the SG soliton:[4,10]

$$\sigma_0=\frac{g^2}{32\pi^2}\int((\partial_3\varphi_{\mathrm{cl}})^2+2m^2\cos(\varphi_{\mathrm{cl}}))dx_3=\frac{g^2m}{2\pi^2}.$$

In S_{eff} all higher-order corrections, coming from tree-level diagrams, were ignored. However, if terms which would contribute to higher curvature corrections are ignored, it is possible to re-sum an infinite subset of the terms which were previously ignored. This can be achieved by considering a domain wall solution which is curved; unfortunately, such configurations are not solutions of the SG equations of motion. They can, on the other hand, be considered as a constraint solution[11] — the solution of the equations of motion with a source term proportional to the argument of the delta function in (4). This can be included in the action by introducing a Lagrange multiplier field. For slowly varying f this equation can be solved by perturbation theory in the derivatives of f. If only the first derivatives of f are taken into account (i.e., ignoring higher curvature corrections), the solution can be constructed by the following simple arguments.[2] When one neglects higher derivatives this implies that f is a linear function of its arguments, which corresponds to the plane domain wall rotated through an angle θ with $\tan\theta=\sqrt{G}$, where $G\equiv 1+(\boldsymbol{\nabla}f)^2$. The classical solution in this case is obtained from (3) by rotation:

$\varphi(x)=\varphi_{\rm cl}((x_3-f)/\sqrt{G})$. This solution is exact in the approximation of constant ∇f, since no source term is required to produce it. Consequently, the Lagrange multiplier appears only in the next order of the derivative expansion and is proportional to $\nabla^2 f$. The effective action with the above solution is equal to the area of the domain wall. The rotated wall area element contains the factor $1/\cos\theta=\sqrt{G}$, and the re-summed effective action is therefore

$$S_{\rm eff}=\sigma_0\int d^2\mathbf{x}\,\sqrt{G(\mathbf{x})}. \tag{6}$$

Since G is the determinant of the induced metric on the string world sheet, we have obtained the Nambu–Goto action.

The next term in the derivative expansion will be of order of the Lagrange multiplier squared, that is $(\nabla^2 f)^2$, and will depend on the choice of the constraint. This arbitrariness leads to an ambiguity in the coefficient of this term, which in the covariant description corresponds to the extrinsic curvature squared. It appears that the area term (6) is the only universal part of the effective action. This is not surprising, since the parameter of the derivative expansion is k/m, where k is a momentum of the excitation on the string world sheet. Higher derivative terms become important when $k\sim m$, i.e., when the wavelength of the excitation is of the same order of the thickness of the domain wall. Such excitations are of course indistinguishable from the fluctuations of the SG field in the bulk. As such, including such fluctuations in the effective string action leads to ambiguities. Of course, the computation of any physical quantity must be invariant under any choice of the constraint. It is the Faddeev–Popov determinant which cancels the ambiguities arising in the bosonic sector of the theory — the full effective action contains the fermionic ghosts coming from the determinant.

The universality of the Nambu–Goto term stems from the rotational invariance of the original model. This holds even when quantum corrections are included as long as the constraint respects rotational symmetry. Constraints which do not respect this symmetry would produce actions that are not reparametrization invariant. We have explicitly checked that when the kernel in (4) is chosen to be $K(\mathbf{x},x_3-f)=\varphi'_{\rm cl}(x_3-f)$, which is not rotationally invariant, the one-loop correction to the constant and to the $(\nabla f)^2$ terms in (6) disagree.

Let us now consider the quantum corrections. The string tension gains quantum corrections from fluctuations of the domain wall and of the field φ in the bulk. To study how these two corrections are correlated we calculate the one-loop corrections to the string tension. The parameter of the loop expansion, m/g^2, is small since m^2 is proportional to the monopole density. These corrections will be computed in the background field method starting from the classical solution (3). The one-loop corrections in 3D SG theory are linearly divergent, which leads to ambiguities in the definition of dimensional quantities like the string tension. However, the monopole gas representation implies the particular UV regularization based on the normal-ordering prescription. To implement this prescription in the background field method, it is instructive to first study the one-loop corrections to the general classical solution. Expanding the quantum field as $\varphi=\varphi_{\rm cl}+\eta$ and integrating out η, we obtain:

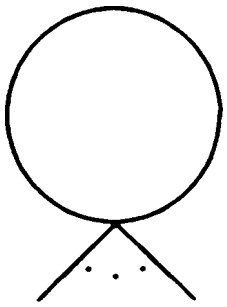

FIG. 1. Tadpole diagrams to be subtracted in the normal-ordering prescription.

$$S_1^{\text{bare}} = \frac{1}{2}\ \mathrm{Tr}\ln\left(\frac{-\partial^2 + m^2\cos\varphi_{\text{cl}}}{-\partial^2 + m^2}\right).$$

The expansion of S_1 in the powers of φ_{cl} yields the usual Feynman diagrams, while the normal-ordering prescription consists in throwing out bubble diagrams (Fig. 1). Thus, to one-loop, the normal ordering is implemented by adding the following counter-term to the effective action:

$$S_1 = \frac{1}{2}\ \mathrm{Tr}\ln\left(\frac{-\partial^2 + m^2\cos\varphi_{\text{cl}}}{-\partial^2 + m^2}\right) - \frac{m^2}{2}\int d^3x(\cos\varphi_{\text{cl}} - 1)\int \frac{d^3p}{(2\pi)^3}\,\frac{1}{p^2+m^2}. \qquad (7)$$

This expression is free of all UV divergences. Notice that since the expansion of the renormalized effective action S_1 begins with φ_{cl}^4 terms, the mass of the photon does not acquire quantum corrections at one loop.

The spectrum of the operator describing the excitations of the soliton are well known. It consists of plane waves in the x_1 and x_2 directions; while the x_3 spectrum is gapped, possessing a zero mode and then a set of continuum states corresponding to the scattering of plane waves off the potential given by the solitonic solution. Inserting the analytic form of the spectrum into (7) we find that the one-loop correction to the string tension is,

$$\Delta\sigma_1 = \frac{1}{2}\int \frac{d^3p}{(2\pi)^3}\ln(p^2+m^2)\,\nu(p_3)$$

$$+\frac{1}{2}\int \frac{d^2p}{(2\pi)^2}\ln(\mathbf{p}^2) + 2m\int \frac{d^3p}{(2\pi)^3}\,\frac{1}{p^2+m^2} = -\frac{m^2}{4\pi}. \qquad (8)$$

Here $\nu(p_3)$ is the difference of the density of scattering states in the presence and absence of the kink, and can be obtained using the exact eigenmodes of the linearized SG equation:[12]

$$\nu(p_3) = \int dx_3(\psi^*_{p_3}(x_3)\psi_{p_3}(x_3) - 1) = -\ \frac{2m}{p_3^2+m^2}.$$

The first term in (8) corresponds to the trace over continuum states; the second term corresponds to the quasi-zero mode contribution; and the last term is the counter-term prescribed by normal ordering. The sum of these three terms is UV finite, although each term diverges individually. This leaves room for some ambiguity in the final finite result depending on what regularization scheme is implemented. However, if the sum of the terms is placed under one single integral, so that the function being integrated over has finite UV behavior, the answer must be regularization independent. The difficulty in implementing such a scheme is that the quasi-zero mode is a 2D integral, while all others are 3D. It is possible to integrate out the p_3 component of the 3D integrals first, which then leaves a single two-dimensional integral to perform. This is the scheme that was used in (8).

Thus far, we have shown that after including one-loop effects the string tension in the SG model is

$$\sigma = \frac{g^2 m}{2\pi^2}\left(1 - \frac{\pi}{2}\frac{m}{g^2}\right).$$

We performed analogous calculation for φ^4 theory with the potential $\lambda(\varphi^2 - m^2/\lambda)^2/2$, the result is

$$\sigma = \frac{4}{3}\frac{m^3}{\lambda}\left(1 - \frac{9}{32\pi}(4 - \ln 3)\frac{\lambda}{m}\right).$$

As mentioned earlier, different regularization schemes will lead to different final answers. The authors of Ref. 13 performed similar calculation s on the φ^4 theory using the zeta-function regularization. That computation, however, did not include the integral over the quasi-zero branch of the theory, and therefore corresponds to obtaining the one-loop correction to the effective string tension rather than the one-loop renormalized string tension. Excluding that branch still leads to finite results in their regularization scheme since it is insensitive to power like divergences. Unfortunately, it yields an answer incompatible with the ansatz of first integrating out p_3 and then performing the finite integrals. This is to be expected, since the quasi-zero branch should and must contribute to the renormalized string tension.

In the preceding, all modes were including in computing the determinant. However, it is possible to integrate out only the scattering states, i.e., to omit the second term in (8), and obtain an effective action for the quasi-zero branch (as in Ref. 13). This branch contains the modes responsible for shifting the surface in the x_3 direction. Omitting the second term in 8 is equivalent to keeping f fixed and integrating out only bulk modes. The one-loop correction with only bulk modes included is badly UV divergent and is not regularization independent. In the naive cutoff regularization the effective string tension for the f fields will be $\sim\Lambda^2\ln(\Lambda^2/m^2)$, as can be easily checked from (8). Of course, hard modes (with $k \gg m$) of the field f cancel this divergence, rendering the physical string tension finite. The implication is that the one-loop renormalization of the string tension is known precisely, even though all the interaction terms are not known.

To summarize we have argued that the accuracy of the macroscopic description of the confining string in compact QED is limited by the fact that the string is not infinitely thin. As a consequence the higher-derivative terms in the world-sheet action are not

universal. Formally, it is possible to obtain an effective string theory action by integrating out φ in (4) exactly. However, the world-sheet action will be scheme dependent and must be supplemented by the fermionic ghosts coming from the constraints. In addition, the action contains rather peculiar divergences and the finite physical quantities obtained from such an effective action appear only after delicate cancellations between these divergences and the contribution of hard modes of the string coordinates.

It is worth mentioning that the derivation of the effective domain wall action by collective coordinate method in one-dimension lower would lead to essentially the same conclusions. In the 2D theory, which can be thought of as a high-temperature reduction of the 3D theory,[14] domain walls correspond to soliton paths. Solitons in 2D SG theory are known to be described by a local field theory, the Thirring model[15] and soliton operators[16] look very much like the dimensional reduction of the Wilson loops (2),[14] the only difference being a local factor rendering the solitons fermionic. Fermion propagators have a well defined sum-over-path representation where the action is the supersymmetrized length of the world line. Nevertheless, at weak SG coupling, solitons cannot be described by the world-line theory, since the four-fermion interaction in the Thirring model, which corresponds to a contact interaction in the sum-over-path picture, becomes infinitely strong.

We are grateful to K. Selivanov and A. Zhitnitsky for discussions. This work is supported in part by NSERC of Canada, a NATO Science Fellowship and, in part, by RFFI Grant 98-01-00327.

[1] D. Jasnow, Rep. Prog. Phys. **47**, 1059 (1984).
[2] R. K. P. Zia, Nucl. Phys. B: Field Theory Stat. Syst. **251[FS13]**, 676 (1985).
[3] G. Münster, Nucl. Phys. B **340**, 559 (1990); G. Münster, http://xxx.lanl.gov/abs/hep-th/9802006.
[4] A. M. Polyakov, Nucl. Phys. B **120**, 429 (1977).
[5] G. 't Hooft, Nucl. Phys. B **79**, 276 (1974); A. M. Polyakov, JETP Lett. **20**, 194 (1974).
[6] A. M. Polyakov, Nucl. Phys. B **486**, 23 (1997).
[7] T. H. R. Skyrme, Proc. Roy. Soc. F **262**, 237 (1961); Nucl. Phys. **31**, 556 (1962); J. K. Perring and T. H. R. Skyrme, Nucl. Phys. **31**, 550 (1962).
[8] J. L. Gervais and B. Sakita, Phys. Rev. D **11**, 2943 (1975); J. L. Gervais, A. Jevicki, and B. Sakita, Phys. Rev. D **12**, 1038 (1975).
[9] J. L. Gervais, A. Jevicki, and B. Sakita, Phys. Rev. D **12**, 1038 (1975); E. Tomboulis, Phys. Rev. D **12**, 1678 (1975).
[10] N. J. Snyderman, Nucl. Phys. B **218**, 381 (1983).
[11] I. Affleck, Nucl. Phys. B **191**, 429 (1981).
[12] J. Goldstone and R. Jackiw, Phys. Rev. D **11**, 1486 (1975).
[13] R. V. Konoplich, Nucl. Phys. B **323**, 660 (1989).
[14] N. O. Agasyan and K. Zarembo, Phys. Rev. D **57**, 2475 (1998).
[15] S. Coleman, Phys. Rev. D **11**, 2088 (1975).
[16] S. Mandelstam, Phys. Rev. D **11**, 3026 (1975).

Published in English in the original Russian journal. Edited by Steve Torstveit.

Squeezed states of light pulses in the presence of a self-effect in an inertial nonlinear medium

F. Popesku and A. S. Chirkin*
M. V. Lomonosov Moscow State University, 119899 Moscow, Russia

(Submitted 26 February 1999)
Pis'ma Zh. Éksp. Teor. Fiz. **69**, No. 7, 481–485 (10 April 1999)

A systematic theory of the formation of squeezed states during the propagation of coherent light pulses in a medium with an inertial Kerr nonlinearity is developed. It is established that the region of the spectrum where the quadrature fluctuations are weaker than the shot noise depends on both the relaxation time of the nonlinearity and the magnitude of the nonlinear phase shift. It is also shown that the frequency at which suppression of the fluctuations is greatest can be controlled by adjusting the phase of the pulse.
 [S0021-3640(99)00407-7]

PACS numbers: 42.50.Dv, 42.65.Tg

In the present letter we analyze the effect of the response time of the cubic nonlinearity of a medium on the formation of nonclassical (squeezed) light. The formation of quadrature-squeezed light as a result of the self-effect of a light pulse is studied. This process, together with the generation of optical solitons and parametric amplification during pulsed pumping, serves as an efficient method for producing pulsed squeezed light. The self-effect of ultrashort laser pulses has been used in Refs. 1–4 for producing squeezed states of light. At the same time, all of the theoretical calculations[4–6] in connection with the analysis of the formation of nonclassical light in the presence of the self-effect of pulses assume that the nonlinear response of the medium is instantaneous and that the relative fluctuations are small. The latter assumption is, of course, valid for the intense pulses ordinarily used in experiments. It should be expected that the response time of the nonlinearity will determine the region of the spectrum of the quantum fluctuations that play a large role in the formation of squeezed light. The point is that even though the frequency band of the pulse is limited, the spectrum of the quantum fluctuations of the pulse is unlimited (in the present-day theory). However, in order to take the nonlinear response time of the medium into account it is necessary to develop an appropriate algebra of time-dependent Bose operators. We have developed such an algebra, and this has made it possible to develop a consistent theory of the formation of nonclassical light as a result of the self-effect of light pulses with no restrictions on their intensity and on the ratio between the relaxation time τ_r of the nonlinearity and the pulse duration τ_p. We present below the results for $\tau_p \gg \tau_r$. We underscore that even in this case this problem cannot be solved correctly without taking the finite relaxation time into account.

The process under consideration is described by an interaction Hamiltonian of the form

$$\hat{H}_{int}=\hbar\beta\int_{-\infty}^{\infty}dt\int_{-\infty}^{t}H(t-t_1)N[\hat{n}(t,z)\hat{n}(t_1,z)]\,dt_1, \tag{1}$$

where the coefficient β is determined by the nonlinearity of the medium, $H(t)$ is the nonlinear response function of the medium ($H(t)\neq 0$ for $t\geqslant 0$ and $H(t)=0$ for $t<0$; a Kerr-type the nonlinearity is assumed), N is the normal-ordering operator, $\hat{n}(t,z)=A^{+}(t,z)A(t,z)$ is the photon number ''density'' operator, and $A^{+}(t,z)$ and $A(t,z)$ are the Bose operators creating and annihilating photons in a given cross section z of the medium at a given time t (see, for example, Ref. 6). The operator $\hat{n}(t,z)$ commutes with the Hamiltonian (1) and therefore $\hat{n}(t,z)=\hat{n}(t,z=0)=\hat{n}_0(t)$, where $z=0$ corresponds to the entrance into the nonlinear medium.

In accordance with Eq. (1) the spatial dynamics of the operator $A(t,z)$ is described by the equation

$$\frac{\partial A(t,z)}{\partial z}+i\beta q[\hat{n}_0(t)]A(t,z)=0, \tag{2}$$

which follows from the Heisenberg evolution equation, where

$$q[\hat{n}_0(t)]=\int_{-\infty}^{\infty}h(t_1)\hat{n}_0(t-t_1)\,dt_1 \qquad (h(t)=H(|t|)).$$

Equation (2) is written in the traveling coordinate system: $z=z$ and the time $t=t'-z/u$, where t' is the running time and u is the velocity of the pulse in the medium. The solution of Eq. (2) is

$$A(t,z)=\exp[-i\gamma q[\hat{n}_0(t)]]A_0(t). \tag{3}$$

Here $A_0(t)=A(t,0)$, $\gamma=\beta z$. For $h(t)=2\delta(t)$ and $A_0(t)=a_0$ expressions (2) and (3) assume a form corresponding to single-mode (monochromatic) radiation. The following commutation relations should hold for arbitrary distances $z\neq 0$:

$$[A(t_1,z),A^{+}(t_2,z)]=\delta(t_1-t_2), \quad [A(t_1,z),A(t_2,z)]=0. \tag{4}$$

To check the relations (4) and to calculate the quantum statistical characteristics of a pulse we developed an algebra of time-dependent Bose operators. Specifically, we obtained the commutation relation

$$A_0(t)\exp[-i\gamma q[\hat{n}_0(t_1)]]=\exp[-i\gamma q[\hat{n}_0(t_1)]-i\gamma h(t_1-t)]A_0(t) \tag{5}$$

and the normal-ordering formula

$$\exp[-i\gamma q[\hat{n}_0(t)]]=N\exp\left\{\int_{-\infty}^{\infty}[\exp(-i\gamma h(\theta_1))-1]\hat{n}_0(t-\theta_1)\,d\theta_1\right\}. \tag{6}$$

Here time is normalized to the nonlinearity relaxation time τ_r, i.e., $\theta=t/\tau_r$. Relations (5) and (6) are a generalization of the well-known relations for the single-mode case.[7]

The photon number operator remains unchanged in the presence of a self-effect. This fact has already been used in Eq. (2). For this reason, in the presence of a self-effect it is of greatest interest to study the fluctuations of the quadrature components. Let us consider the quadrature component

$$\hat{X}(t,z)=\frac{1}{2}[A^{+}(t,z)+A(t,z)]. \tag{7}$$

The correlation function of the quadrature fluctuations $\hat{X}(t,z)$

$$R(t,t+\tau)=\frac{1}{2}[\langle\hat{X}(t,z)\hat{X}(t+\tau,z)\rangle+\langle\hat{X}(t+\tau,z)\hat{X}(t,z)\rangle-2\langle\hat{X}(t,z)\rangle\langle\hat{X}(t+\tau,z)\rangle] \tag{8}$$

(the brackets denote averaging over the quantum state of the pulse) is given by the expression

$$R(t,t+\tau)=\frac{1}{4}\{\delta(\tau)-\psi(t)h(\tau)\sin 2\Phi(t)+\psi^{2}(t)g(\tau)\sin^{2}\Phi(t)\}, \tag{9}$$

where $\psi(t)=2\gamma|\alpha_0(t)|^2$ is the nonlinear phase shift, $\alpha_0(t)$ is an eigenvalue of the operator $A_0(t)$ of a pulse in a coherent state, $\Phi(t)=\psi(t)+\phi(t)$ ($\phi(t)$ is the initial phase of the pulse), $\delta(\tau)$ is a delta function, and $g(\tau)=\tau_r^{-1}(1+|\tau|/\tau_r)\exp(-|\tau|/\tau_r)$ for the nonlinearity relaxation response under study, $h(\tau)=\tau_r^{-1}\exp(-|\tau|/\tau_r)$. The derivation of Eq. (9) took into consideration the facts that the nonlinear phase shift per photon $\gamma\ll 1$ and that the relaxation time is much shorter than the pulse duration ($\tau_r\ll\tau_p$).

In accordance with Eq. (9) the spectral density of the quadrature fluctuations is

$$S(\omega,t)=\int_{-\infty}^{\infty}R(t,t+\tau)e^{i\omega\tau}d\tau$$

$$=\frac{1}{4}[1-2\psi(t)L(\omega)\sin 2\Phi(t)+4\psi^{2}(t)L^{2}(\omega)\sin^{2}\Phi(t)], \tag{10}$$

where $L(\omega)=1/[1+(\omega\tau_r)^2]$. It follows from Eq. (10) that, depending on the value of the phase $\Phi(t)$, the quadrature fluctuation can be weaker or stronger than the shot noise corresponding to the coherent state of the pulse, $S^{(\mathrm{coh})}(\omega)=\frac{1}{4}$. In accordance with the Heisenberg uncertainty relation, the behavior of the spectrum in the conjugate quadrature is shifted in phase by $\pi/2$.

If the phase of the pulse is chosen optimal for a frequency ω_0,

$$\phi_0(t)=\frac{1}{2}\tan^{-1}[(\psi(t)L(\omega_0))^{-1}]-\psi(t), \tag{11}$$

the spectral density at this frequency is

$$S(\omega_0,t)=\frac{1}{4}[\sqrt{1+\psi^{2}(t)L^{2}(\omega_0)}-\psi(t)L(\omega_0)]^{2} \tag{12}$$

and increases monotonically with the phase $\psi(t)$.

For arbitrary frequency ω we have

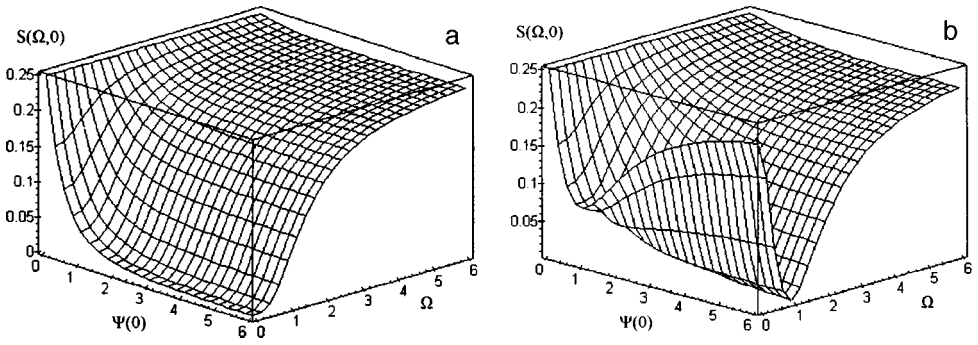

FIG. 1. Dispersion of the fluctuations of the quadrature component of a pulse at time $t=0$ as a function of the maximum nonlinear phase $\psi(0)=2\gamma|\alpha_0(0)|^2$ and the reduced frequency $\Omega=\omega\tau_r$ at values of the phase of the pulse which are optimal for $\Omega=0$ (a) and $\Omega=1$ (b).

$$S(\omega,t)=S(\omega_0,t)+\frac{1}{2}[L(\omega)-L(\omega_0)]\psi(t)\{[L(\omega)+L(\omega_0)]\psi(t)$$

$$-[1+(L(\omega)+L(\omega_0))L(\omega_0)\psi^2(t)][1+\psi^2(t)L^2(\omega_0)]^{-\frac{1}{2}}\}. \qquad (13)$$

The spectra calculated using Eq. (13) at $t=0$ for $\omega=0$ and $\omega=\tau_r^{-1}$ are presented in Fig. 1. It is evident from Fig. 1a that for $\omega_0=0$ the spectral density of the fluctuation s is minimum at the frequency $\omega=0$ for any value of the phase $\psi(0)$. For $\omega_0\neq 0$ (Fig. 1b) and phases $\psi(0)>1$ the minimum of the fluctuation spectrum lies at frequencies $\omega=\tau_r^{-1}$ and for $\psi(0)<1$ the minimum lies near $\omega\approx 0$. It is also obvious from Figs. 1a and 1b that the frequency band in which the spectral density of the quadrature fluctuations is lower than the shot noise level depends on the nonlinear phase shift $\psi(0)$. The corresponding dependence for $\omega_0=0$ is displayed in Fig. 2, whence it follows that for $\psi(0)\gg 1$ the width of the spectrum below the shot noise level is 1.5 times greater than the width of the spectral response of the nonlinearity.

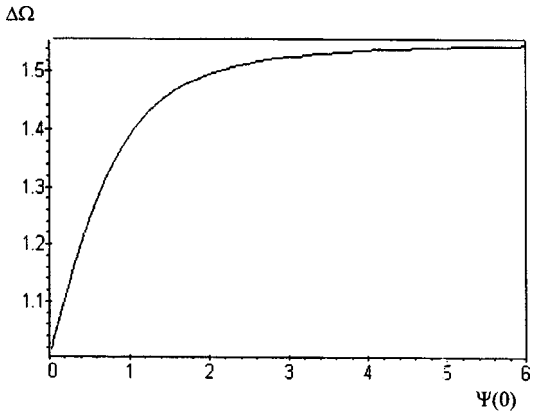

FIG. 2. Spectral band $\Delta\Omega=2\Delta\omega\tau_r$ (at half-height) of the quadrature of a pulse with suppressed quantum fluctuations as a function of the maximum nonlinear phase $\psi(0)$.

The results obtained in the present letter can be used to analyze correctly the experiments of Refs. 1–4, in which laser pulses with a duration of the order of 100 ps and quartz optical fibers were used and the maximum nonlinear phase shift ψ was greater than 1. Of course, in measurements of the quadrature spectrum the suppression of quantum fluctuations of a pulse will be smoothed out (see Eq. (13)). This time over which ''smoothing out'' occurs in the case of balanced homodyne detection[8] is determined by the duration of the heterodyne pulse.

The theory developed makes it possible to optimize the strategy for producing and detecting ultrashort pulses in a squeezed state. Quantum fluctuations of short pulses are ordinarily measured at high frequencies of the order of several tens of MHz in order to avoid any effects due to technical fluctuations concentrated at low frequencies. However, as a rule, the suppression of quantum fluctuations is greatest in this region. Our results show that by adjusting the phase of the signal pulse (or, generally speaking, the phase of the heterodyne pulse), one can achieve maximum suppression of the fluctuations specifically at the spectral component of interest to us. We underscore once again that this spectral component can lie on the wing of the spectral response of the nonlinearity (Fig. 1b). This means that nonlinear media with a longer relaxation time and correspondingly a larger nonlinearity can be used to obtain squeezed-light pulses.[6]

In closing, we note that the approach developed in the present letter can be used to analyze the formation of polarization-squeezed light in media with a cubic nonlinearity[9,10] and to develop a quantum theory of nonlinear matching devices[11] for pulsed signals.

We thank K. N. Drabovich for helpful discussions of this work.

This work was supported in part by the Russian Fund for Fundamental Research (Grant No. 96-02-16714) and the program ''Fundamental Metrology'' of the Government Committee on Science and Technology.

*e-mail: chirkin@foton.ilc.msu.su

[1] M. Rosenbluh and R. M. Shelby, Phys. Rev. Lett. **66**, 153 (1991).
[2] K. Bergman and H. A. Haus, Opt. Lett. **16**, 663 (1991).
[3] N. Nishizawa, S. Kume, M. Mori *et al.*, Jpn. J. Appl. Phys., Part 1 **33**, 138 (1994).
[4] N. Nishizawa, M. Hashiura, T. Horio *et al.*, Jpn. J. Appl. Phys., Part 2 **37**, L792 (1998).
[5] M. Shirasaki and H. A. Haus, J. Opt. Soc. Am. B **7**, 30 (1990).
[6] S. A. Akhmanov, V. A. Vysloukh, and A. S. Chirkin, *Optics of Femtosecond Laser Pulses*, AIP, 1992 [Supplemented translation of Russian original, Nauka, Moscow, 1988].
[7] W. H. Louisell, *Radiation and Noise in Quantum Electronics*, McGraw-Hill, New York, 1964; Nauka, Moscow, 1972.
[8] U. Leonhardt, *Measuring the Quantum State of Light*, Cambridge University Press, New York, 1997.
[9] A. S. Chirkin, A. A. Orlov, and D. Yu. Parashchuk, Kvant. Élektron. (Moscow) **20**, 999 (1993).
[10] A. P. Alodzhants, S. M. Arakelyan, and A. S. Chirkin, Zh. Éksp. Teor. Fiz. **108**, 63 (1995) [JETP **81**, 34 (1995)]; Quantum Semiclassic. Opt. **9**, 311 (1997).
[11] N. Korol'kova and J. Perina, Opt. Commun. **136**, 135 (1997).

Translated by M. E. Alferieff

On harmonic generation in a photoionized gas

V. P. Silin

P. N. Lebedev Physics Institute, Russian Academy of Sciences, 117924 Moscow, Russia

(Submitted 10 February 1999; resubmitted 23 February 1999)
Pis'ma Zh. Éksp. Teor. Fiz. **69**, No. 7, 486–490 (10 April 1999)

The laws characterizing the radiation of high harmonics due to the coherent bremsstrahlung effect are indicated in the limit of high intensity of the laser pump photoionizing a gas in regime of suppression of the ionization barrier. It is shown that the intensity of the harmonics is determined by the quantum properties of the electron distribution in an atom before it is ionized. © *1999 American Institute of Physics.* [S0021-3640(99)00507-1]

PACS numbers: 42.65.Ky, 52.40.Nk

The generation of high harmonics of optical radiation has been attracting a great deal of attention in the last few years, both as a general problem of nonlinear optics and as a problem whose solution opens up prospects for many applications.[1] The study of the generation of very high harmonics started with plasma as the nonlinear medium.[2,3] In the last few years harmonic generation has been studied in neutral gases (see, for example, Refs. 4 and 5). However, as the lasers employed are improved and the energy flux density of the laser radiation increases, neutral gases become ionized.[6–8] Thus attention once again turns to plasma as a nonlinear medium for generating high harmonics of laser radiation. There is a tendency in experiments to increase the intensity of the laser radiation when photoionization is the process used to ionize the gas.

In this letter we present the basic laws characterizing the efficiency of harmonic generation in a photoionized plasma, which are determined by the quantum distribution of electrons in an atom. The exposition is mainly of a qualitative nature and is based on an associative generalization of the existing results of the theory of harmonic generation in a preprepared classical plasma. In what follows we shall concentrate on the limit of a pump field which is strong enough that photoionization occurs under conditions of suppression of the ionization barrier (SIB).[9,10] In so doing, first, we shall assume the ionization potential I_i of the atoms to be small compared with the energy $(1/2)mV_E^2$ of the electron oscillations in the pump electric field $E(t)=E\cos\omega t$, where $V_E=|eE/m\omega|$ is the amplitude of the oscillatory electron velocity and e and m are the electron charge and mass, respectively. This means that the Keldysh parameter of the theory of tunneling ionization is small: $\gamma=(2I_i/mV_E^2)^{1/2}\ll 1$ (Ref. 11). Second, we shall assume the parameter $\beta=(1/16Z)(I_i/I_{\rm H})^2(E_{\rm at}/E)$ to be small. Here Z is the nuclear charge of the atom, $I_{\rm H}$ is the ionization potential of the hydrogen atom, and $E_{\rm at}=5.13\times 10^9$ V/cm is the atomic unit of electric field intensity. In the case of interest here, where $\beta<1$, according to Refs. 9 and 10 an electron is ionized from an atom without tunneling. In other words, photo-

ionization in the SIB model is determined by the free, virtually unimpeded, escape of an electron from an atom. For a spatially uniform distribution of atoms in a plasma this makes it possible to express the electron momentum distribution function in the form $f(\mathbf{p},t)=F(\mathbf{p}-m\mathbf{u}(t))$. Here $\mathbf{u}(t)$ is the time-dependent electron velocity in the electric field of the laser pump ionizing the atoms. This form of the electron distribution is similar to that ordinarily arising in the theory of harmonic generation in a plasma in the first collisionless approximation.[2] However, in the present case, in a coordinate system oscillating together with the electron it is the electron momentum distribution inside an atom before the radiation acts on the plasma. For a pure quantum state, to within a normalization factor,

$$F(\mathbf{p})=\sum_q |a_q(\mathbf{p})|^2,$$

where $a_q(\mathbf{p})$ is the electron wave function in the momentum representation and the summation extends over all quantum numbers corresponding to the electron distribution inside the atom. Such a distribution is physically obvious. It can also be obtained directly by using the equation for the density matrix in the Wigner representation[12] (see below).

The similarity so arising and, at the same time, the obvious difference between the cases of a preprepared plasma and a photoionized plasma in the SIB regime makes it possible to establish the following general law characterizing the generation efficiency $\eta^{(2l+1)}$ of the $(2l+1)$-st harmonic due to coherent bremsstrahlung (compare Refs. 2 and 13–15):

$$\eta^{(2l+1)}=(q^{(2l+1)}/q)=\{[\nu(V)/\omega]h(l)S([2l+1][V/V_E])\}^2, \tag{1}$$

where $q^{(2l+1)}$ and q are, respectively, the energy flux density of the $(2l+1)$-st harmonic and the pump. In Eq. (1) the function $\nu(V)$ is the electron-velocity-dependent electron–ion collision frequency, which corresponds to the cause responsible for the harmonic generation — bremsstrahlung due to the oscillatory motion of the electrons in the Coulomb field of the ions, and $h(l)$ is a function of the number of the harmonic and in the case of a plane-wave geometry for both the pump and generated harmonic fields is given by[13–15]

$$h(l)=[l(l+1/2)^2(l+1)]^{-1}.$$

Finally, the function S, which is determined by the electron distribution inside the atom, depends in the high-field regime $V_E \gg V$ on the argument $([2l+1]V/V_E)$, where V is the characteristic electron velocity for some electron velocity distribution that does not take braking effects into account. This is similar to the results obtained in Refs. 13–15, and it can also be established directly for the photoelectron distribution in the SIB regime (see below).

In order to use our general expression (1) to examine the quantum properties of the efficiency of harmonic generation in a photoionized plasma we shall first use the expression for the electron–ion collision frequency corresponding to the Fokker–Planck–Landau collision integral $\nu(V)=4\pi e^2 e_i^2 n_i \Lambda/m^2V^3$, where $e_i=Z_i|e|$ is the ion charge, n_i is the ion number density, and Λ is the Coulomb logarithm. For ionization in the SIB

regime it is natural to take $V=V_Z$, where $V_Z=Ze^2/\hbar$ is the Coulomb unit of velocity,[16] and Z is the nuclear charge of an atom, as distinct from Z_i, which is the multiplicity of ionization. Then

$$\frac{\nu(V_Z)}{\omega}=3\Lambda\frac{Z_i^2e^4m}{\hbar^2(\hbar\omega)}\left[\frac{4\pi}{3}\frac{\hbar^6}{m^3Z^3e^6}n_i\right]=3\Lambda\left(\frac{Z_i}{Z}\right)^2\frac{2I_Z}{\hbar\omega}O_Zn_i,$$

where $I_Z=Z^2I_{\rm H}$, $I_{\rm H}$ is the ionization potential of a hydrogen atom, $O_Z=(4\pi/3)a_Z^3$, and $a_Z=\hbar^2/Ze^2m$ is the Coulomb unit of length.[16] Using $a=\hbar^2/e^2m\cong0.53\times10^{-8}$ cm, we write Eq. (1) in the form

$$\eta^{(2l+1)}\cong1.43\times10^{-5}[h(l)]^2\frac{Z_i^4}{Z^6}\left(\frac{I_{\rm H}}{\hbar\omega}\right)^2\left(\frac{\Lambda}{10}\right)^2(n_i[20])^2\left\{S\left([2l+1]\frac{V_Z}{V_E}\right)\right\}^2, \qquad (2)$$

where $n_i[20]$ is the ion number density in units of 10^{20} cm^{-3}. For what follows it is helpful to write down in a similar form an expression for the energy flux density q (W$\cdot$cm^{-2}) of the pump radiation:

$$q=\frac{c}{8\pi}E^2=\frac{Z}{16\pi}\frac{V_E^2}{V_Z^2}\left(\frac{\hbar\omega}{I_Z}\right)^2\frac{cI_Z}{a_Z^3}=3\times10^{16}\left(\frac{V_E}{V_Z[2l+1]}\right)^2Z^2\left(l+\frac{1}{2}\right)^2\left(\frac{\hbar\omega}{I_{\rm H}}\right)^2.$$

The maximum value of the efficiency $\eta^{(2l+1)}$ corresponds to the maximum value of the function $S(x)=S_m$, which occurs at $x=x_m$. Substituting the corresponding numbers into the formulas gives both the maximum generation efficiency of the $(2l+1)$-st harmonic and the corresponding flux density of the pump.

Before illustrating the general laws presented above, determined by the quantum properties of electrons in an atom, let us note that the main equation for the theory of harmonic generation that determines the pump-induced electron current density $\delta\mathbf{j}$, characterizing the coherent bremsstrahlung of a plasma, is most easily obtained by using the quantum density matrix in the Wigner representation.[12] This equation has the form

$$\frac{\partial\delta\mathbf{j}}{\partial t}=-\frac{4\pi e^2e_i^2n_i\Lambda}{m^2}\frac{en_im^2}{(2\pi\hbar)^2}\sum_q\int d\mathbf{r}_1d\mathbf{r}_2\frac{(\mathbf{r}_1-\mathbf{r}_2)}{|\mathbf{r}_1-\mathbf{r}_2|^2}\{\sin[(m\mathbf{u}_E(t)/\hbar)(\mathbf{r}_1-\mathbf{r}_2)]$$
$$\times[\psi_q(\mathbf{r}_1)\psi_q^*(\mathbf{r}_2)+\psi_q^*(\mathbf{r}_1)\psi_q(\mathbf{r}_2)]-\cos[(m\mathbf{u}_E(t)/\hbar)(\mathbf{r}_1-\mathbf{r}_2)]$$
$$\times[\psi_q(\mathbf{r}_1)\psi_q^*(\mathbf{r}_2)-\psi_q^*(\mathbf{r}_1)\psi_q(\mathbf{r}_2)]\}.$$

Here $\psi_q(\mathbf{r})$ is the wave function of an electron in an atom before it is ionized. This function corresponds to the full set of quantum numbers q characterizing the electronic state. It should be stressed here that the electronic states of an atom have a substantial influence on the source current for harmonic generation. This has not been appreciated at all in the theory of coherent bremsstrahlung generation of harmonics in plasma (see, for example, the review Ref. 15).

Let us illustrate the above for the photoionization of the $1s$ state of a hydrogenlike atom, where

$$S(x)=(x^3/4\pi)\{E_1(x)+[(4/3)+(x/3)]e^{-x}\},\quad E_1(x)=\int_x^\in(dt/t)e^{-t}. \qquad (3)$$

According to Eq. (2), the function (3) describes harmonic generation over a wide range of pump intensities. For this function $S_m=0.28$ at $x_m=3.34$. Among other things, this makes it possible to find from Eqs. (2) and (3) the maximum efficiency, the corresponding pump intensity, and the energy flux density of the $(2l+1)$-st harmonic:

$$\eta_{m,1s}^{(2l+1)}\approx 10^{-6}[h(l)]^2(Z_i^4/Z^6)(I_{\rm H}/\hbar\omega)^2(\Lambda/10)^2(n_i[20])^2,$$

$$q_{m,1s}(2l+1)\approx 2.7\times 10^{15}Z^2(l+1/2)^2(\hbar\omega/I_{\rm H})^2 W\cdot\ {\rm cm}^{-2},$$

$$q_{m,1s}^{(2l+1)}=q_{m,1s}\eta_{m,1s}^{(2l+1)}=\frac{2.7\times 10^9(n_i[20])^2}{[l(l+1/2)(l+1)]^2}\left(\frac{\Lambda}{10}\right)^2\left(\frac{Z_i}{Z}\right)^4 W\cdot{\rm cm}^{-2}.$$

Applying the latter formulas to a photoionized helium plasma for $\hbar\omega\simeq 4$ eV pump radiation and assuming $\Lambda=10$ and $n_i[20]=10$ for the generation of the 63rd harmonic, which corresponds to the optical transmission window of water, I obtain $q_{m,1s}(63)=10^{18}\ {\rm W\cdot cm}^{-2}$ and $q_{m,1s}^{(63)}=280\ {\rm W\cdot cm}^{-2}$.

In conclusion, I note that an accurate memory of the electron distribution in an atom is lost at times greater than the transit time

$$t_{ee}(V_Z)=\frac{m^2V_Z^3}{4\pi e^4\Lambda n_e}=\frac{\tau_a}{3\Lambda n_e O_Z}\cong\left(\frac{10}{\Lambda}\right)\frac{Z^3}{Z_i n_i[20]}\ 13\times 10^{-15}\ {\rm s}.$$

Here $\tau_a=\hbar^3/e^2m\simeq 2.42\times 10^{-17}$ s is the atomic unit of time, and the relation $n_e=Z_in_i$ between the electron and ion number densities is taken into account. For helium $t_{ee}\cong 5\times 10^{-15}$ s. For long times the relaxation to a Maxwell distribution does not break the quantum scaling (1) and (2) of the dependence on the number of the harmonic, which goes over to the classical temperature scaling of Ref. 14. Only changes of unit order in the coefficients arise. The latter occurs over a comparatively long time interval. This important property is due to the important circumstance that electron–ion collisions are suppressed by a strong electromagnetic field,[2] and therefore the electron heating time is much longer than t_{ee}. For this reason, for a long time the electron ''temperature'' corresponds to the quantum energy of electron motion in the atom.

In summary, we have established new laws characterizing the generation of high harmonics in a plasma photoionized by high-power radiation under conditions of suppression of the ionization barrier (conditions which are discussed here for the first time), such that a memory of the quantum electron distribution in the atom determines the properties of the harmonic radiation.

This work was performed under the Government Program for Support of the Leading Scientific Schools (No. 96-15-96750), INTAS (Project No. 97-0369), and the Russian Fund for Fundamental Research (Project No. 99-02-18075).

[1] S. M. Gladkov and N. I. Koroteev, Usp. Fiz. Nauk **160**(7), 105 (1990) [Sov. Phys. Usp. **23**, 554 (1990)].
[2] V. P. Silin, Zh. Éksp. Teor. Fiz. **47**, 2254 (1964) [Sov. Phys. JETP **20**, 1510 (1965)].
[3] N. H. Burnett, H. A. Baldis, M. C. Richardson, and G. D. Enright, Appl. Phys. Lett. **31**, 172 (1977).
[4] A. L'Huillier, K. J. Schafer, and K. C. Kulander, J. Phys. B **24**, 3315 (1991).
[5] C. Altucci, T. Starczewski, E. Mevel *et al.*, J. Opt. Soc. Am. B **13**, 148 (1996).
[6] J. L. Krause, K. J. Schafer, and K. C. Kulander, Phys. Rev. Lett. **68**, 3335 (1992).
[7] C.-G. Wahlstrom, J. Larsson, A. Persson *et al.*, Phys. Rev. A **48**, 4709 (1993).
[8] K. Kondo, T. Tamida, Y. Nabekawa, and S. Watanabe, Phys. Rev. A **49**, 3881 (1994).

[9] S. Augst, D. D. Meyerhofer, D. Strickland, and S. L. Chin, J. Opt. Soc. Am. B **8**, 858 (1991).
[10] M. V. Fedorov and J. Peatross, Phys. Rev. A **52**, 504 (1995).
[11] L. V. Keldysh, Zh. Éksp. Teor. Fiz. **47**, 1945 (1964) [Sov. Phys. JETP **20**, 1307 (1965)].
[12] V. P. Silin, *Introduction to the Kinetic Theory of Gases*, FIAN Press, Moscow, 1998.
[13] V. P. Silin, Zh. Éksp. Teor. Fiz. **114**, 864 (1998) [JETP **87**, 468 (1998)].
[14] K. N. Ovchinnikov and V. P. Silin, Sb. KSF FIAN, No. 10, 19 (1998).
[15] V. P. Silin, Kvant. Elektron. (Moscow) **26**, 11 (1999).
[16] L. D. Landau and E. M. Lifshitz, *Quantum Mechanics: Non-Relativistic Theory*, 2nd ed., Pergamon Press, Oxford, 1965 [Russian original, GIFML, Moscow, 1963].

Translated by M. E. Alferieff

Interference of two Bose–Einstein condensates

V. A. Alekseev*
P. N. Lebedev Physics Institute, Russian Academy of Sciences, 117924 Moscow, Russia

(Submitted 2 December 1998; resubmitted 26 February 1999)
Pis'ma Zh. Éksp. Teor. Fiz. **69**, No. 7, 491–496 (10 April 1999)

The visibility of the density interference pattern of two Bose–Einstein condensates, which are produced in traps and overlap after the trapping potential is switched off, is investigated. Coherent wave packets are used to describe the order parameter in a second-quantization formalism. This results in a decrease of the visibility of the interference fringes with increasing time delay between the formation of the condensates and the observation of interference. In the two limiting cases of ideal and very dense gases the correlation time increases, $\tau\to\infty$, and the result is identical to that obtained using an approach based on the Gross–Pitaevskiĭ equation. Under the conditions of the experiment performed by M. R. Andrews, C. G. Townsend, H. J. Miesner *et al.*, Science **275**, 6367 (1997), the computed correlation time $\tau\approx 0.2$ s is much longer than the confinement time of the condensate, and it is possible to observe the predicted decrease of visibility of the interference fringes of the density of the atoms. © *1999 American Institute of Physics.* [S0021-3640(99)00607-6]

PACS numbers: 03.75.Fi, 03.75.Dg

Experiments were recently performed to observe the density interference between two Bose condensates.[1] Atoms trapped in a magnetic trap were spatially separated into two groups by a laser beam and cooled. Then the trapping potential was switched off and the condensates expanded and overlapped. The interference fringes of the atomic densities were observed in the overlap region.

In both the initial assumption in setting up this experiment[2] and the theoretical description following the experiment[3,4] the authors initially conjectured that the atomic density interference fringes are formed as a result of the appearance of an order parameter (or a macroscopic wave function of the condensate) $\Psi(x)=\langle\hat{\Psi}(x)\rangle$, which means that invariance under $U(1)$ gauge transformations breaks down. The wave function of the condensate is a solution of the nonlinear Schrödinger equation in which the interatomic interaction is assumed to be a contact interaction and the $\hat{\Psi}$ operator is replaced by a c-number, $\hat{\Psi}(x)\to\Psi(x)$.[5,6] It is supposed that such an equation, called the Gross–Pitaevskiĭ equation (GPE), completely describes the state of the system at temperature $T=0$. Then there is no need to use the second-quantization formalism.

At the same time such a description of interference is not the only possible one. The

assumption that a nonzero value $\langle\hat{\Psi}(x)\rangle\neq 0$ is formed is actually equivalent to the assumption that the condensate wave function is a superposition of states $|N\rangle$ with different numbers N of particles. We suppose that this superposition has the form of a coherent wave packet, used by Anderson to describe superfluidity,[7]

$$\Psi=\sum_N A_N|N\rangle, \quad A_N=\pi^{-1/4}\Delta N^{-1/2}\exp\left\{-\frac{(N-\overline{N})}{2\Delta N^2}+iN\varphi\right\}, \tag{1}$$

where φ is a phase.

The main assertion of the present letter is as follows. The use of the state (1) to describe interference results in a new qualitative result that does not occur in the GPE approach — a decrease of the visibility of the interference pattern with increasing time delay between the formation of the state (1) and the observation of the interference. According to our estimates, such a decrease of visibility can be observed under the conditions of the experiment of Ref. 1. Descriptions using the states (1) and on the basis of the GPE lead to the same results only in the two limiting cases of an ideal gas and a very dense gas (in the latter case the correlation time increases very slowly, $\tau\sim N^{1/10}$, and such conditions are virtually impossible to obtain). Since in the GPE approach essentially nothing is known about the dynamics of the formation of both the state (1) and the macroscopic wave function, at present only experiments can show which description is the correct one.

Two possible formulations of an interference experiment are examined. In an experiment of the first type (I), which was realized in Ref. 1, a magnetic trap containing trapped atoms is divided by a laser beam into two halves, which are cooled to a condensate state, after which the trapping potential is switched off and the condensates overlap. In the second case (II), which was also discussed in Ref. 1, but which thus far has not been realized as far as we know, a trap with the atoms cooled to a condensate state is divided in half and after a time delay the trapping potential is switched off.

Following Ref. 4, we shall use the Wigner function

$$W(x,p,t)=\frac{1}{2\pi}\int \exp\left(-i\frac{py}{\hbar}\right)\left\langle\hat{\Psi}^+\left(x+\frac{y}{2}\right)\hat{\Psi}\left(x-\frac{y}{2}\right)\right\rangle dy, \tag{2}$$

where the brackets indicate averaging over the condensate state, to describe the interference of the condensates.

In the GPE approach there is no need for such averaging. In this case $\hat{\Psi}(x)$ is a c-number,

$$\Psi(x)=\psi_\alpha(x)\sqrt{N_\alpha}\exp\left(-\frac{i}{\hbar}\mu_\alpha t\right)+e^{i\varphi}\psi_\beta(x)\sqrt{N_\beta}\exp\left(-\frac{i}{\hbar}\mu_\beta t\right), \tag{3}$$

where $\psi_{\alpha,\beta}$ are the solutions of the nonlinear Schrödinger equation for each of the traps α and β, with particle numbers $N_{\alpha,\beta}$ and chemical potentials $\mu_{\alpha,\beta}$, and φ is a phase. The average assumes the form

$$\langle\hat{\Psi}^+(x)\hat{\Psi}(x')\rangle=\sum_{i,k=\alpha,\beta} g_{ik}\psi_i^*(x)\psi_k(x'), \tag{4}$$

$$g_{\alpha\alpha}=N_\alpha, \quad g_{\beta\beta}=N_\beta, \quad g_{\alpha\beta}=g^*_{\beta\alpha}=\sqrt{N_\alpha N_\beta}\exp\left(\frac{i}{\hbar}(\mu_\alpha-\mu_\beta)t+i\varphi\right). \tag{5}$$

For an ideal gas, after the potential is switched off $W(x,p,t)$ satisfies the Liouville equation, whence it is easy to conclude[4] that density interference fringes form with visibility $V=2|g_{\alpha\beta}|/(g_{\alpha\alpha}+g_{\beta\beta})$. For $N_\alpha=N_\beta=N/2$ Eq. (5) gives $V=1$. A numerical solution of the GPE showed[3] that the interaction of the particles changes the structure of the fringes, but the visibility is once again equal to unity.

When the second-quantization formalism is employed, at $T=0$ only the ground-state functions of the traps $\hat{\Psi}(x)=\hat{a}_\alpha\psi_\alpha(x)+\hat{a}_\beta\psi_\beta(x)$ need be retained in the field operator. Then expression (4) retains its form, but the correlation function is equal to the average, $g_{ik}=\langle a_i^+ a_k\rangle$, and Eq. (5) changes. Otherwise, everything said about interference remains in force.

A solution of the form (3) of the GPE is the only possible solution at $T=0$. An attempt to represent it as a superposition of the states (3) with different N_α and N_β is admissible only for an ideal gas. For a gas of interacting particles the particle number dependence of the chemical potential would lead to temporal oscillations of both the average total number of particles and the number of particles in each condensate. Therefore, irrespective of the method used to produce condensates, the visibility in the GPE approach equals unity, $V=1$, and does not depend on the time. The situation is different when N-states and wave packets are used.

The calculation of an average value with the standard state $|N_\alpha,N_\beta\rangle$, corresponding to a fixed number of particles in each condensate, leads to the result $g_{\alpha\beta}=\langle a_\alpha^+ a_\beta\rangle=0$, i.e., interferen ce vanishes. However, as was noted in Ref. 8, for the method used to cool the atoms there are no grounds for assuming that the condensate state is a state with a fixed number of particles. Let us assume, for example, that at the final stage of cooling the wave function of N atoms in a trap is a superposition of the states $|N,0,\dots\rangle$, corresponding to N atoms in the ground state, and $|N-1,1,0,\dots\rangle$, corresponding to $N-1$ atoms in the ground state and one atom in the first excited state. The cooling rf field removes an excited atom from the trap, switching the state $|N-1,1,0,\dots\rangle$ into $|N-1,0,\dots\rangle$. As a result, the final state is a superposition of states with N and $N-1$ particles. It is obvious that in the general case, as a result of such a process, the state of the condensate at $T=0$ is described by a superposition of functions $|N,0,\dots\rangle\equiv|N\rangle$ with different N. We shall assume that this superposition is of the form (1).

Following Anderson,[7] we shall assume that the amplitudes A_N have a sharp maximum at $N=\overline{N}$ with variance $\Delta N^2\approx\overline{N}$. In this case, the weak dependence of the functions $|N\rangle$, which are a solution of the GPE (or the equivalent Hartree–Fock equation), on the number N of particles can be neglected in the field operator, and we can set $|N\rangle=|\overline{N}\rangle$. We then obtain from Eq. (1) the value

$$\langle\hat{\Psi}\rangle=\langle\hat{a}\rangle|\overline{N}\rangle=\sum_N A_{N-1}A_N\sqrt{N}e^{(i/\hbar)(E_{N-1}-E_N)t+i\varphi}|\overline{N}, \tag{6}$$

which is identical to the solution of the GPE, if in Eq. (6) the small difference in the coefficients $A_{N-1}\approx A_N$ is neglected and it is assumed that $\sqrt{N}=\sqrt{\overline{N}}$, while the energy difference between the states is represented approximately in the form E_N-E_{N-1}

$=\partial E/\partial N=\mu(\overline{N})$, neglecting the next higher-order terms in the expansion (in the case of an ideal gas the next higher-order terms are absent and the result becomes exact). Taking the next term in the expansion into account and replacing the summation by integration, we obtain

$$\langle\hat{a}\rangle=\sqrt{\overline{N}}\exp\left[-(t/\tau)^2-i\frac{\mu}{\hbar}t+i\varphi\right],\quad \tau=2\hbar/\Delta N s,\quad s=\partial\mu/\partial N. \tag{7}$$

In a type-I experiment, where the condensates are cooled independently, we obtain $\langle\hat{a}_\alpha\hat{a}_\beta^+\rangle=\langle\hat{a}_\alpha\rangle\langle\hat{a}_\beta^+\rangle$, whence

$$g_{\alpha\beta}=\langle\hat{a}_\alpha\rangle\langle\hat{a}_\beta^+\rangle=\sqrt{\overline{N}_\alpha\overline{N}_\beta}\exp\left[-\left(\frac{t}{\tau_\alpha}\right)^2-\left(\frac{t}{\tau_\beta}\right)^2-i\frac{\mu_\alpha-\mu_\beta}{\hbar}t+i(\varphi_\alpha-\varphi_\beta)\right]. \tag{8}$$

Hence one can see that the correlation function and, correspondingly, the visibility of the interference pattern decrease with increasing time interval t between the formation of a coherent wave packet (1) and the observation of the interference fringes. The correlation time τ can be estimated by setting $\Delta N=\sqrt{\overline{N}}$.

For a rarefied gas the correction introduced to the energy $E(N)$ of the ground state of the system by the interaction of the particles can be calculated in the standard manner as $\Delta E(N)=\langle N|U|N\rangle$, where

$$U=U_0\hat{a}_0^+\hat{a}_0^+\hat{a}_0\hat{a}_0,\quad U_0=\frac{2\pi a\hbar^2}{m}\int|\psi_0|^4d\mathbf{r}=q\hbar\overline{\omega},$$

m is the mass of an atom, a is the scattering length, ψ_0 is the ground state function in a parabolic trap, $\overline{\omega}=(\omega_x+\omega_y+\omega_z)/3$ is the average frequency of the trap, and $q=\sqrt{2/\pi}(a/R)\sqrt{(\omega_x\omega_y\omega_z)/\overline{\omega}^3}$, with $R=\sqrt{\hbar/(m\overline{\omega})}$. Finally, $E(N)=\hbar\overline{\omega}(3N/2+qN^2)$. Naturally, in such a calculation the interaction is assumed to be weak: $qN\sim aN/R\ll 1$. Hence we find $\partial\mu/\partial N=\partial^2E/\partial N^2=2\hbar\overline{\omega}q$ and $\tau\approx\omega^{-1}(\overline{N})^{-1/2}q^{-1}$.

For $qN\gg 1$ the Thomas–Fermi approximation[9,10] can be used to calculate the chemical potential, $\mu=\frac{1}{2}\hbar\omega(15\overline{N}a/R)^{2/5}$, whence $\tau\approx\omega^{-1}q^{-2/5}\overline{N}^{1/10}$.

Thus, as particle number increases, the correlation time at first decreases as $\sim N^{-1/2}$, reaches a minimum $\tau\sim\omega^{-1}q^{-1/2}\sim 0.03$ s at $N\sim 10^3$ (under the conditions of Ref. 1, $\omega\sim 10^3$ s^{-1} and $q\sim 10^{-3}$), and then increases very slowly as $\tau\sim 0.05N^{1/10}$ s. Formally, in the limit $N\to\infty$ we obtain $\tau\to\infty$, and Eq. (8) becomes identical to the GPE result (5). Under the experimental conditions of Ref. 1, however, $N\sim 10^6$, which is very far from this limit, and $\tau\approx 0.2$ s. This time is much longer than the overlap time ~ 0.04 s of the condensates after the potential is switched off, but much shorter than the confinement time ~ 30 s of the condensate state. Thus there arises the question of what to use as the time origin in Eq. (8), which is unsatisfactory from this standpoint. We also note that if the phases in the superposition (1) are arbitrary, then the result is much less than that obtained from Eq. (8). An experimental investigation of the dependence of the visibility of the fringes on the time delay between the formation of a condensate and the switching off of the potential can shed light on this situation. We note that the replacement of

summation over N by integration in the derivation of Eq. (7) suppressed the correlation function revivals resulting from the revival of the order parameter, which was discussed in Ref. 11.

We shall now discuss the type-II experiment, where the condensate formed in a trap is divided into two parts and the potential is switched off after a time delay τ. To describe this experiment there is no need to assume $U(1)$ violation.

Neglecting particle interaction before the division, the wave function of N atoms can be written in the form $\Psi(x_1,\ldots,x_N)=\psi_0(x_1)\ldots\psi_0(x_N)$, where $\psi(x)$ is the ground-state wave function of the trap. After the division this function assumes the form

$$\Psi(x_1\ldots x_N)=\tilde{\psi}(x_1)\ldots\tilde{\psi}(x_N),\quad \tilde{\psi}(x)=c_\alpha\psi_\alpha(x)+c_\beta\psi_\beta(x), \tag{9}$$

$$c_\alpha=\sqrt{\lambda},\quad c_\beta=\sqrt{1-\lambda}e^{i\varphi},\quad 0<\lambda<1.$$

The coefficient λ and the phase φ reflect the possible asymmetry of the division process. Next, it is important to represent the ground state (9) $|\tilde{N}=N\rangle=(N!)^{-1/2}(c_\alpha\hat{a}_\alpha^+ + c_\beta\hat{a}_\beta^+)^N|0\rangle$ as a superposition of the states $|N_\alpha,N_\beta\rangle=(N_\alpha!N_\beta!)^{-1/2}(a_\alpha^+)^{N_\alpha}\times(a_\beta^+)^{N_\beta}|0\rangle$ with N_α and N_β particles in each condensate. Calculating the matrix element

$$\langle N_\alpha,N_\beta|\tilde{N}=N\rangle=c_\alpha^{N_\alpha}c_\beta^{N_\beta}\sqrt{\frac{N!}{N_\alpha!N_\beta!}}\delta_{N_\beta,N-N_\alpha},$$

we find the wave function of the two condensates

$$|\tilde{N}=N\rangle=(c_\alpha c_\beta)^n\sum_k\left(\frac{c_\alpha}{c_\beta}\right)^k\sqrt{\frac{N!}{(n+k)!(n-k)!}}|n+k,n-k\rangle,\quad n=N/2. \tag{10}$$

The superposition (10), like (1), is a wave packet, but the phases of the constituent states are determined by the division process.

We now note that for $c_\alpha\approx c_\beta\approx 1/\sqrt{2}$ (the condensate is divided into two approximately equal parts) the terms in Eq. (10) have a sharp maximum at $k=0$. In this case the function (10) is also applicable for interacting particles, if the functions $\psi_{\alpha,\beta}$ are taken to be the solutions of the Hartree–Fock (or GPE) equation with $N_\alpha=N_\beta=N/2$ particles.

Next, it is necessary to take into account the relation

$$\langle n+k,n-k|\hat{a}_\alpha^+\hat{a}_\beta|n+k',n-k'\rangle=\delta_{k',k-1}\sqrt{(n+k)(n-k+1)}e^{(i/\hbar)Q(k)t},$$

where $Q(k)$ is the difference of the energies of the states, which it is convenient to write in the form

$$Q(k)=\mu_\alpha-\mu_\beta+S(k-1/2),\quad S=\partial\mu_\alpha/\partial n+\partial\mu_\beta/\partial n=s_\alpha+s_\beta. \tag{11}$$

Then all sums appearing in the calculation of the average $\langle\hat{a}_i^+\hat{a}_k\rangle$ over the state (10) can be calculated exactly, and we find

$$g_{ii}=N_i|c_i|^2,\quad g_{\alpha\beta}(N)=Nc_\beta c_\alpha^* e^{(i/\hbar)(\mu_\alpha-\mu_\beta)t}(|c_\beta|^2e^{(-i/2\hbar)St}+|c_\alpha|^2e^{(i/2\hbar)St})^{N-1}. \tag{12}$$

When the initial state of the condensate is described by the wave packet (1), the correlation function (12) must also be averaged over N. A calculation shows that this

leads to an additional time dependence, but a much slower one than that in Eq. (12). In other words, in this case the description of the initial state of the condensate (before the division) by a wave function with a fixed number of particles leads to the same results as the description using a wave packet.

For equal number of particles in the condensates $|c_\alpha|^2=|c_\beta|^2=1/2$ the visibility $V(t)=|\cos(St/2\hbar)|^{N-1}$ corresponding to Eq. (12) decreases from 1 at $t=0$ to 0 in a characteristic time $t>\tau\approx 2\hbar/S\sqrt{N}$. With trivial modifications the same estimates are valid for the correlation time τ as in the case I after Eq. (8). We underscore, however, that in the case II the time t is determined uniquely: It is the time delay between the moment when the condensate is divided and the moment when the potential is switched off.

At times which are multiples of $\tau_1=4\pi 2\hbar/S$, as one can see from Eq. (12), interference is revived. The visibility of the revived pattern is close to the initial visibility, except when the two conditions $qN\gg 1$ and $|\mu_\alpha-\mu_\beta|\sim\mu_{\alpha,\beta}$ hold simultaneously, in which case it is suppressed by the term quadratic in k, which was neglected in the expansion (11).

The method for obtaining the wave function (10) is similar in many respects to that used in Ref. 12, but in Ref. 12 the authors arrive at a different result. They assert that the time delay leads only to diffusion of the phase of the interference pattern, which randomly fluctuates in different realizations of an experiment with the same time delays.

The decrease in the visibility and the revival of the interference pattern do not fit into the GPE approach. The experimental observation or proof of the absence of these phenomena could increase substantially our understanding of the process leading to the formation of and the properties of condensate states.

It is our pleasure to thank A. F. Andreev for helpful discussions.

This work was supported in part by the Russian Fund for Fundamental Research under Grant No. 98-02-17502 and by the Government Science and Engineering Program ''Metrologiya.''

*e-mail: valeks@sci.lebedev.ru

[1] M. R. Andrews, C. G. Townsend, H. J. Miesner *et al.*, Science **275**, 637 (1997).
[2] W. Hoston and L. You, Phys. Rev. A **53**, 4254 (1996).
[3] A. Rohrl, M. Naraschewski, A. Schenzle *et al.*, Phys. Rev. Lett. **78**, 4143 (1997).
[4] H. Wallis, A. Rohrl, M. Naraschewski *et al.*, Phys. Rev. A **55**, 2109 (1997).
[5] E. P. Gross, Nuovo Cimento **20**, 454 (1961).
[6] L. P. Pitaevskiĭ, Zh. Éksp. Teor. Fiz. **40**, 646 (1961) [Sov. Phys. JETP **13**, 451 (1961)].
[7] P. W. Anderson, Rev. Mod. Phys. **38**, 298 (1966).
[8] A. F. Andreev, JETP Lett. **63**, 1018 (1996).
[9] V. V. Goldman, I. F. Silvera, and A. J. Leggett, Phys. Rev. B **24**, 2870 (1981).
[10] D. A. Huse and E. D. Siggia, J. Low Temp. Phys. **46**, 137 (1982).
[11] E. M. Wright, D. F. Walls, and J. C. Garrison, Phys. Rev. Lett. **77**, 2158 (1996).
[12] J. Javanainen and M. Wilkens, Phys. Rev. Lett. **78**, 4675 (1997).

Translated by M. E. Alferieff

Andreev reflections and magnetoresistance in ferromagnet–superconductor mesoscopic structures

V. I. Fal'ko and C. J. Lambert
School of Physics and Chemistry, Lancaster University, LA1 4YB, UK

A. F. Volkov
School of Physics and Chemistry, Lancaster University, LA1 4YB, UK;
Institute of Radio Engineering and Electronics, 117454 Moscow, Russia

(Submitted 23 February 1999)
Pis'ma Zh. Éksp. Teor. Fiz. **69**, No. 7, 497–502 (10 April 1999)

An analysis is made of the change in the resistance of a nanostructure consisting of a diffusive ferromagnetic (F) wire and normal metal electrodes, due to the onset of superconductivity (S) in the normal electrode and Andreev scattering processes. The superconducting transition results in an additional contact resistance arising from the necessity to match the spin-polarized current in the F-wire to the spinless current in the S reservoir, which is comparable to the resistance of a piece of F wire with length equal to the spin relaxation length. It is also shown that in the absence of spin relaxation the resistance of a two-domain structure is the same for a ferro- or antiferromagnetic configuration if one electrode is in the superconducting state.
 [S0021-3640(99)00707-0]

PACS numbers: 73.23.−b, 75.70.Pa, 74.80.Dm

In recent years studies of transport in mesoscopic conductors with strongly correlated electrons have revealed a number of novel phenomena, including the occurrence of a giant magnetoresistance (GMR) in multilayer FN structures,[1] where F(N) are ferromagnetic (normal) metals. At the same time a variety of new transport properties arising from superconductivity (S) in mesoscopic NS structures have been identified.[2,3] More recently the effect of superconductivity on the transport properties of spin-polarized electrons in magnetic materials was studied[4–8] and it was observed that the onset of superconductivity may lead to an increase or decrease of the conductance of an F film.[4–6] This change may be as much as 10% of the normal state conductance and is too large to be attributed to the superconducting proximity effect (in magnetic materials, such as Ni and Co, the exchange energy ϵ_{ex} is two orders of magnitude larger than the superconducting gap Δ, which suppresses the proximity effect).

It has been pointed out by de Jong and Beenakker[9] that if the conductivities $\sigma_{\uparrow}$ and $\sigma_{\downarrow}$ for spin-up and spin-down electrons in a ferromagnetic material are different, then the resistance of a ferromagnetic wire increases due to contact with a superconductor. This is because the electrical current in the *s*-wave superconductor is spinless, and matching the spin-polarized current in the ferromagnet to the spinless current in the S reservoir in-

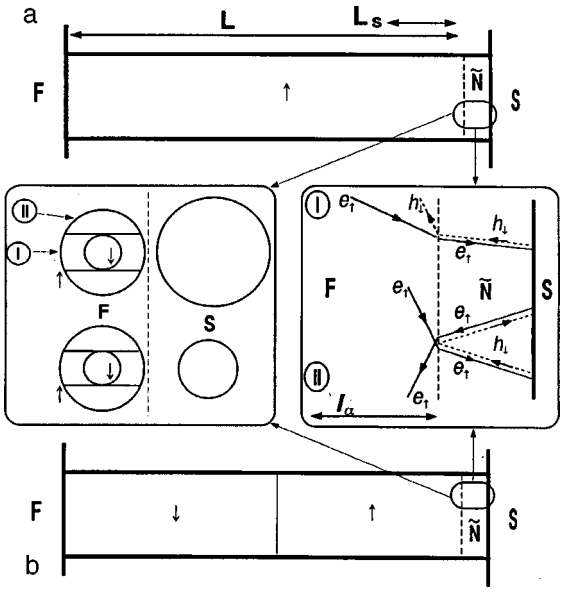

FIG. 1. Pictorial representation of the two-domain FS structure with ferromagnetic (a) and antiferromagnetic (b) alignment of domains, a double Andreev reflection process in it, and of possible relations between Fermi surfaces of spin-up and -down electrons in the F wire (left) and in the N(S) metal (right).

volves the Andreev scattering process, which increases the resistance of a system. When the ferromagnetic wire is long and when spin relaxation processes in it are efficient, the resistance variation of a diffusive FS structure caused by this mechanism has the form of an additional contact resistance[10] of the FS interface, which can be also extended onto multiterminal geometry.[11] The necessity to match the spinless and spin-polarized currents at the FS interface also results in a different nonequilibrium population of spin-up and -down states near the superconducting contact (within one spin relaxation length L_s).

In the present paper, we consider a nanostructure consisting of a ferromagnetic wire with one ($F_{\uparrow\uparrow}$) or two anti-collinear ($F_{\uparrow\downarrow}$) domains embedded between two normal reservoirs , one of which becomes superconducting at $T=T_c$. The sequence of domains in a ferromagnetic wire represents our simplified view of a multilayer GMR structure. We calculate the resistances of these structures,[1)] $R_{\uparrow\uparrow N}$, $R_{\uparrow\downarrow N}$, $R_{\uparrow\uparrow S}$ and $R_{\uparrow\downarrow S}$ in the limit of a long and short spin relaxation length ($L_s \gg L$, $L_s \ll L$) and in the case when the FS interface itself causes the spin relaxation (for example, due to spin–orbit coupling). We find that, in the absence of spin relaxation, $R_{\uparrow\uparrow N} < R_{\uparrow\downarrow N} = R_{\uparrow\uparrow S} = R_{\uparrow\downarrow S}$, so that an applied magnetic field (which polarizes domains) yields a nonzero resistance variation above T_c, as in typical giant magnetoresistance systems, and gives no resistance variation at $T \ll T_c$. Spin relaxation processes of any kind (either due to spin–orbit coupling in the bulk of a ferromagnetic metal and its surface, or caused by a noncollinearity of ferromagnetic domains in the wire) change the resistance $R_{\uparrow\uparrow S}$, leading to a nonzero magnetoresistance at $T<T_c$.

First of all, we consider the structure $F_{\uparrow\uparrow}$N(S) shown in Fig. 1a, which consists of a single ferromagnetic domain. The resistance of a disordered F wire can be found by

solving diffusion equations for the isotropic part of the electron distribution function, $n_\alpha(z,\varepsilon)=\int d\Omega_{\mathbf{p}} n_\alpha(z,\mathbf{p})$. Using the electron–hole symmetry, we restrict our analysis to the calculation of a symmetrized function $N_\alpha(\varepsilon,z)=1/2[n_\alpha(z,\varepsilon)+n_\alpha(z,-\varepsilon)]$, where ε is determined with respect to the chemical potential in the S(N) electrode. In terms of $N_\alpha(\varepsilon,z)$, the electric and spin current densities are given by

$$j_{Q,M}=j_\alpha \pm j_{\bar{\alpha}}, \quad j_\alpha=\sigma_\alpha \int_{-\infty}^{\infty} \frac{d\varepsilon}{e} \partial_z N_\alpha(\varepsilon,z), \tag{1}$$

where $\bar{\alpha}=(\downarrow,\uparrow)$ for $\alpha=(\uparrow,\downarrow)$, and $\sigma_\alpha=e^2\nu_\alpha D_\alpha$, where ν_α and D_α are the density of states and diffusion coefficient for electrons in the spin state α. The functions $N_\alpha(\epsilon,z)$ obey the diffusion equation

$$D_\alpha \partial_z^2 N_\alpha(z,\varepsilon)=w_{\uparrow\downarrow}\nu_{\bar{\alpha}}[N_\alpha(z,\varepsilon)-N_{\bar{\alpha}}(z,\varepsilon)], \tag{2}$$

which is more convenient to use in the equivalent form

$$\partial_z^2 \sum_{\alpha=\uparrow\downarrow} D_\alpha \nu_\alpha N_\alpha=0, \; [\partial_z^2-L_s^{-2}](N_\uparrow-N_\downarrow)=0. \tag{3}$$

The term on the right-hand side of Eq. (2) accounts for spin relaxation, which may result from both spin–orbit or spin-flip scattering at defects. It can be used to define the effective spin relaxation length, L_s as $L_s^{-2}=w_{\uparrow\downarrow}[\nu_\uparrow/D_\downarrow+\nu_\downarrow/D_\uparrow]$. This pair of equations, which ignore any energy relaxation, should be complemented by four boundary conditions, two on each side of the ferromagnetic wire.

The boundary conditions for Eqs. (2) and (3) can be obtained in various ways. We employ the model shown in Fig. 1, where the FS junction is replaced by a sandwich of three layers: (i) a ferromagnetic (F) wire of length L connected to the bulk F reservoir, (ii) a normal metal layer ($\tilde{\mathrm{N}}$) which never undergoes a superconducting transition by itself and has a negligible resistance, and (iii) a bulk electrode S(N) which undergoes the superconducting transition. The insertion of a normal metal layer $\tilde{\mathrm{N}}$ between the F and S(N) parts allows us to formulate the boundary conditions at the FS interface using known boundary conditions at the $\tilde{\mathrm{N}}$S interface.[3] For the sake of simplicity, we consider $\tilde{\mathrm{N}}$ to be ballistic and the F$\tilde{\mathrm{N}}$ junction to be semiclassically transparent, so that electrons either pass from one side to the other, or are fully reflected, depending on whether this process is allowed by energy–momentum conservation near the Fermi surface. The latter approximation avoids resonances through the ''surface states''[12] due to multiple passage through the normal layer inserted between S and F. As illustrated in Fig. 1, we approximate the spectrum of electrons by parabolic bands — two for spin-down and spin-up electrons in F, and one in the N part, which we take into account by introducing the parameters $\delta_{\alpha\mathrm{N}}^2=p_{\mathrm{FN}}^2/p_{\mathrm{F}\alpha}^2$ and $\delta^2=(p_{\mathrm{F}\downarrow}/p_{\mathrm{F}\uparrow})^2<1$. The $\tilde{\mathrm{N}}$N interface is assumed to be ideal, and the Fermi surfaces in $\tilde{\mathrm{N}}$ and N layers to be the same, so that $\tilde{\mathrm{N}}$S Andreev reflection has unit probability. In such a model, the momentum of an electron in the plane of the junction is conserved.

The boundary conditions on the left end are given by the equilibrium distribution of electrons in the F electrode,

$$N_\alpha(-L/2,\varepsilon)=\frac{1}{2}[n_T(\varepsilon-eV)+n_T(-\varepsilon-eV)]. \tag{4}$$

The boundary condition on the other end depends on the state of the electrode, and in the superconducting state takes into account Andreev reflection at the NS interface.[13] Since in our model of an ideal F$\tilde{\text{N}}$ interface, the parallel component of the electron momentum is conserved, the effective reflection/transmission of electrons in parts I and II of the ferromagnet Fermi surface sketched in Fig. 1 are different. Although nonequilibrium quasiparticles from F pass inside $\tilde{\text{N}}$ and generate holes by being Andreev reflected at the $\tilde{\text{N}}$S interface, only those holes which are created by quasielectrons from part I of the Fermi surface in F may escape into the F wire. The spin-down holes which were generated by spin-up electrons from part II of the Fermi surface cannot find states in F, so that they are totally internally reflected into $\tilde{\text{N}}$. Then, they undergo a second Andreev reflection, convert into spin-up electrons, and return back into the ferromagnetic wire. This results in *total internal reflection* of spin-up electrons from part II of the Fermi surface inside the F wire, which nullifies the spin current through its FS edge.

The boundary condition near the F$\tilde{\text{N}}$ junction can be found by matching the isoenergetic electron fluxes determined in the diffusive region found in the ballistic F region using the reflection/transmission relation between the distributions of incident and Andreev or normally reflected electrons. For quasiparticles with energies $0<\varepsilon<\Delta$ this can be written in the form

$$\sigma_\uparrow\partial_z N_\uparrow-\sigma_\downarrow\partial_z N_\downarrow=-s(N_\uparrow-N_\downarrow), \tag{5}$$

$$N_\uparrow+N_\downarrow+\frac{2}{3}\varkappa\delta^2 l_\downarrow\partial_z N_\downarrow=2N_T(\varepsilon), \tag{6}$$

where $\varkappa=(1-\delta^2)^{3/2}/\delta^2$, $\delta^2=p_{\text{F}\downarrow}^2/p_{\text{F}\uparrow}^2<1$, and $N_T(\varepsilon)=1/2[n_T(\varepsilon)+n_T(-\varepsilon)]=1/2$ at $T=0$. The spin relaxation term on the right hand side of Eq. (5) takes into account the spin–orbit relaxation on the FN interface.

One can obtain boundary conditions in another way, after having considered both the F wire and an auxiliary N piece of a normal metal in the diffusive limit, using the known boundary conditions at the NS interface.[3] Then, Eq. (5) follows from the condition $\partial_z f_\alpha=0$ at the NS interface,[3,14] where $f_\alpha=[n_\alpha+(1-n_{\bar{\alpha}}(-\epsilon)]/2$ is the sum of the distribution functions of electrons and holes. Equation (6) emerges from the equilibrium condition for electrons and holes in opposite spin states at the SN interface (if we neglect the third term on the left in Eq. (6) and set the electric potential equal to zero in S). At energies above the superconducting gap Δ, the boundary conditions coincide with Eq. (4).

For a ferromagnetic wire with sufficient intrinsic spin relaxation, $L_s\ll L$, we find that the contact resistance of the FS boundary is equal to

$$r_{\text{c}}^{\text{S}}=R_\square\frac{L_s}{L_\perp}\frac{\varsigma^2}{1-\varsigma^2}+\frac{R_\square l_+}{3L_\perp}\frac{\varkappa}{1+\varsigma}, \tag{7}$$

where $\zeta=(\sigma_\uparrow-\sigma_\downarrow)/(\sigma_\uparrow+\sigma_\downarrow)$ is the degree of spin polarization of a current in a monodomain ferromagnetic wire, $R_\square$ is the resistance per square of a monodomain ferromagnetic film, and $L_\perp$ is the wire width.

In the normal state of the right hand reservoir, the boundary conditions at the end of an F wire depend on the relation between the Fermi momenta of electrons in the ferromagnet and normal metal,

$$N_\alpha(z,\varepsilon)+\frac{4\varkappa_{\alpha\mathrm{N}}D_\alpha}{v_\alpha}\partial_z N_\alpha(z,\varepsilon)\Big|_{z=L/2}=N_T(\varepsilon), \tag{8}$$

where $\varkappa_{\alpha\mathrm{N}}=(1-\delta_{\alpha\mathrm{N}}^2)^{3/2}/\delta_{\alpha\mathrm{N}}^2$, $\delta_{\alpha\mathrm{N}}<1$, and $\varkappa_{\alpha\mathrm{N}}=0$, $\delta_{\alpha\mathrm{N}}\geqslant 1$, $\delta_{\alpha\mathrm{N}}^2=p_{\mathrm{FN}}^2/p_{\mathrm{F}\alpha}^2$. These result in the contact resistance term

$$r_{\mathrm{c}}^{\mathrm{N}}=R_\square\frac{l_+(1+\varsigma)}{L_\perp}\left\{(1-\varsigma)l_+/L_s+\frac{3}{2}\varkappa_{+\mathrm{N}}^{-1}\right\}^{-1}, \tag{9}$$

which has sense only when it is larger than the resistance of a short piece of F wire with length of the order of l_+. Otherwise, it should be neglected.

After comparing the latter result to $r_{\mathrm{c}}^{\mathrm{S}}$, we find that the resistance of a long ferromagnetic wire attached to an S electrode exceeds the resistance of the same wire connected to a normal reservoir by the resistance of an F segment of length of order of L_s. One can extend the result of Eq. (7) to finite temperatures, which yields the resistance variation below the superconducting transition[10]

$$R_{\mathrm{S}}(T)-R_{\mathrm{N}}\approx\frac{\varsigma^2}{1-\varsigma^2}\frac{L_s}{L_\perp}R_\square\tanh\left(\frac{\Delta(T)}{2T}\right). \tag{10}$$

Note that the increase of the resistance in Eq. (10) originates from *the matching of a spin-polarized current in the highly resistive ferromagnetic wire to a spinless current inside the superconductor*. We expect this robust effect to be present both in the monodomain and polydomain wires, with domain size $L_{\mathrm{D}}>L_s$.

The solution of Eqs. (2)–(6) can also be used to describe the contrasting case of a ferromagnetic wire where all spin relaxation processes take place only at the FS interface. Such a structure may consist of either of one or of two ferromagnetic domains with antiparallel magnetizations (antiferromagnetic configuration), as shown Fig. 1b. In the latter case, we neglect the local microscopic $\mathrm{F}_\uparrow\mathrm{F}_\downarrow$ interface resistance, so that the boundary conditions for $N_\alpha(x)$ at the domain wall can be reduced to the continuity equation for the spin current, $\sigma_\alpha\partial_z N_\alpha$ and for the distribution functions N_α. This yields

$$R_{\uparrow\uparrow\mathrm{N}}=\frac{L}{\sigma_\uparrow+\sigma_\downarrow},\quad R_{\uparrow\downarrow\mathrm{N}}=R_{\uparrow\downarrow\mathrm{S}}=\frac{\sigma_\uparrow+\sigma_\downarrow}{4\sigma_\uparrow\sigma_\downarrow}L,$$

and

$$R_{\uparrow\uparrow\mathrm{S}}=\frac{L(\sigma_\uparrow+\sigma_\downarrow+4s(L/2))}{4(\sigma_\uparrow\sigma_\downarrow+s(L/2)(\sigma_\uparrow+\sigma_\downarrow))}. \tag{11}$$

From this, we deduce that the alignment of magnetizations in two domains results in a significant change of the resistance in the case of normal reservoirs (N) and leaves the conductance unchanged when one of the reservoirs is a superconductor if spin relaxation

is completely absent, or the wire is too short: $R_{\uparrow\uparrow S}(sL\to 0)\to R_{\uparrow\downarrow S}$. A similar behavior has been observed in numerical simulations of the transport through the giant magnetoresistance system with S contacts.[15] In a word, when superconducting leads inject a spinless electric current into the spin-conserving multidomain system, the change in the polarization of domains does not affect of resistance of the system. Spin relaxation at the FS surface restores the sensitivity of the system to the polarization state of domains, and in a long wire ($L\to\infty$) the interplay between Andreev scattering and spin relaxation results in a contact resistance, similar to that in Eq. (7):

$$R_{\uparrow\uparrow \mathrm{S}}(T)-R_{\uparrow\uparrow \mathrm{N}}\approx \frac{\mathfrak{s}^2}{2s}\tanh\left(\frac{\Delta(T)}{2T}\right). \tag{12}$$

Note that the electric current generates a nonequilibrium magnetization, $\delta M=\mu(\nu_\uparrow\int d\epsilon N_\uparrow-\nu_\downarrow\int d\epsilon N_\downarrow)$, which is different for different configurations: $\delta M_{\uparrow\uparrow \mathrm{N}}=0$,

$$\delta M_{\uparrow\uparrow \mathrm{S}}=\left(z/L+\frac{1}{2}\right)M_0,\quad \delta M_{\uparrow\downarrow \mathrm{N}}=\delta M_{\uparrow\downarrow \mathrm{S}}=\left(\frac{1}{2}-|z|/L\right)M_0,$$

$$M_0=eV\frac{4\nu_\uparrow\nu_\downarrow}{\nu_\uparrow+\nu_\downarrow}\mathfrak{s}\mu$$

for $T\ll T_c$. Here, μ is the magnetic moment of electrons, $-L/2<z<L/2$, and $z=0$ corresponds to the $F_\uparrow F_\downarrow$ domain wall.

In summary, we have shown that in the absence of any spin relaxation the resistances of the structures $F_{\uparrow\downarrow}N$, $F_{\uparrow\downarrow}S$ and $F_{\uparrow\uparrow}S$ are equal but differ from the resistance of the $F_{\uparrow\downarrow}N$ structure. This can be regarded as a prediction of a suppression of the giant magnetoresistance in multilayer FN structures with superconducting leads and no spin relaxation. Surface spin relaxation at the FS interface alters the equivalence between $R_{\uparrow\uparrow S}$ and $R_{\uparrow\downarrow S}$ resistances. When the spin relaxation is fast in the bulk of the ferromagnetic material, the resistance of the $F_{\uparrow\uparrow}S$ structure changes at the superconducting transition by a contact resistance value which depends on the spin relaxation rate. For example, in a ferromagnetic wire in which the size of a ferromagnetic domain is larger than the spin relaxation length L_s, the resistance variation is formed within the L_s segment of the F wire (where the spin-polarized current from the F part relaxes to a spinless current in S), and $R_S(T)-R_N$ increases from zero at T_c to a positive value at $T=0$.

The authors thank V. Petrashov, R. Raimondi, E. McCann and S. Iordanski for discussions. This work was funded by EPSRC and EC TMR Program.

[1)]The indices ↑(↓) stand for the alignment of the magnetizations of the domains, and S(N) stand for the normal and superconducting states, respectively, of the right-hand reservoir.

[1] M. N. Baibich, J. M. Broto, A. Fert *et al.*, Phys. Rev. Lett. **61**, 2472 (1988);W. P. Pratt, Jr., S.-F. Lee, J. M. Slaughter *et al.*, ibid. **66**, 3060 (1991).
[2] C. W. J. Beenakker, Rev. Mod. Phys. **69**, 731 (1997).
[3] C. Lambert and R. Raimondi, J. Phys.: Condens. Matter **10**, 8 (1998).
[4] V. T. Petrashov, V. N. Antonov, S. V. Maksimov, and R. Sh. Shaikhaidarov, JETP Lett. **59**, 551 (1994); V. T. Petrashov *et al.*, preprint.
[5] H. D. Lawrence and N. Giordano, J. Phys.: Condens. Matter **8**, L563 (1996).
[6] M. Giroud, H. Courtois, K. Hasselbach *et al.*, Phys. Rev. B **58**, 11872 (1998).

[7] V. A. Vasko *et al.*, Phys. Rev. Lett. **78**, 1134 (1997).
[8] S. K. Upadhyay, A. Palanisami, R. N. Louie, R. A. Buhrman, Phys. Rev. Lett. **81**, 3247 (1998).
[9] M. J. M. de Jong and C. W. J. Beenakker, Phys. Rev. Lett. **74**, 1657 (1995).
[10] V. I. Fal'ko, A. F. Volkov and C. Lambert, http://xxx.lanl.gov/abs/cond-mat/9901051.
[11] F. J. Jedema, B. J. van Wees, B. H. Hoving *et al.*, http://xxx.lanl.gov/abs/cond-mat/9901323.
[12] S. Kuplevakhski and Igor I. Fal'ko, JETP Lett. **52**, 957 (1990); Phys. Met. Metallogr. **71**, 68 (1991).
[13] A. F. Andreev, Zh. Exp. Teor. Fiz. **46**, 1823 (1964) [Sov. Phys. JETP **19**, 1228 (1964)].
[14] A. I. Larkin and Yu. N. Ovchinnikov, in *Non-Equilibrium Superconductivity*, edited by D. N. Langenberg and A. I. Larkin, Elsevier, Amsterdam 1986, p. 493.
[15] F. Taddei, S. Sanvito, J. H. Jefferson, and C. J. Lambert, preprint.

Published in English in the original Russian journal. Edited by Steve Torstveit.

Effect of surface magnetism of solid-state substrates on the NMR of liquid ^{3}He

A. V. Klochkov, V. V. Naletov, M. S. Tagirov, and D. A. Tayurskiĭ
Kazan State University, 420008 Kazan, Russia

(Submitted 21 January 1999; resubmitted 24 February 1999)
Pis'ma Zh. Éksp. Teor. Fiz. **69**, No. 7, 503–509 (10 April 1999)

The results of investigations of the longitudinal relaxation rate of the nuclear spins of liquid helium-3 in contact with finely dispersed $LiYF_4$ dielectric powders with various degrees of filling of the microcracks on the crystal surface by water molecules are reported. It is found that exchange correlations appear between paramagnetic defect centers on the surface as a result of spin-density transfer via the molecular orbitals of oxygen in the water molecule. © *1999 American Institute of Physics.* [S0021-3640(99)00807-5]

PACS numbers: 67.55.−s, 76.60.Es, 75.30.Pd

The success of the method of NMR of the nuclei in liquid ^{3}He for investigating the unusual properties of this quantum liquid at low and ultralow temperatures is well known. One such effect is the presence of magnetic coupling of the nuclear spins of liquid helium-3 and the magnetic moments of a solid-state substrate. The nature of this coupling is still not completely understood, even though the effect of the container walls on the magnetic relaxation of spins in liquid helium-3 was observed 40 years ago.[1] In Refs. 2 and 3 it was established reliably that magnetic coupling exists between the nuclear spins of ^{19}F fluorine present in the microspheres of finely dispersed (0.2 μm) DLX-6000 polytetrafluoroethylene powder, and in Ref. 4 transfer of magnetization from the ^{19}F nuclear spins to protons present in polystyrene microspheres via the nuclear spins of liquid helium-3 was observed.

The cross relaxation observed in Ref. 5 between the nuclear magnetic moments of ^{169}Tm in thulium ethylsulfate and the nuclear spins of liquid ^{3}He stimulated the investigation of magnetic coupling between liquid helium-3 and dielectric Van Vleck paramagnets. The magnetic relaxation of liquid ^{3}He in contact with single crystals of the dielectric Van Vleck paramagnet $LiTmF_4$ and its diamagnetic analog $LiYF_4$ was investigated in Ref. 6. It was found that the magnetic relaxation of the nuclear spins of liquid ^{3}He present in the gap between two $LiYF_4$ single-crystal surfaces acquires substantially new features as compared with relaxation in a bulk liquid. Thus, according to the Bloembergen–Purcell–Pound (BPP) theory,[7] at temperatures 1–4 K the longitudinal and transverse relaxation in bulk liquid ^{3}He are governed by the modulation of the dipole–dipole interaction by the diffusive motion and have the same rates, of the order of 10^{-3} s^{-1}. Even though the gap width is macroscopic (10^{-4} m), the experimental results attest to the existence of a large increase in the relaxation rates, and the transverse relaxation

time T_2 of the nuclear spins of liquid helium-3 is much shorter than the longitudinal relaxation time T_1, similarly to the well-known picture of nuclear magnetic relaxation in solids. When one of the diamagnetic $LiYF_4$ crystals was replaced by a crystal of the Van Vleck paramagnet $LiTmF_4$, an even larger increase of the magnetic relaxation rates of liquid helium-3 was observed. It was found that the experimental data cannot be explained on the basis of standard theories of magnetic relaxation, even taking account of the effect of the nuclear magnetic moments of thulium, and a model of the effect of a restricted geometry (microcracks on the crystal surfaces) on the magnetic relaxation was proposed. The basic idea of the proposed model consists in the following. In solids, where there is essentially no translational motion of atoms, the magnetic resonance line is quite wide and the transverse relaxation times are short. In liquids, on account of the translational motion of the atoms the resonance line is strongly narrowed and the relaxation times are long. When a liquid in which the main relaxation mechanism is modulation of the dipole–dipole interaction by diffusive motion is placed in a restricted geometry, in contrast to the case of a bulk liquid not all modes of diffusive motion are possible — only the resonant modes survive. Therefore a magnetic resonance line will not be narrowed as much as in a bulk liquid, and at the same time it will not be as wide as in the case of a solid. For a quantum liquid such as liquid helium-3 there may be even more such limitations, for example, because of the Pauli exclusion principle, on the diffusive motion. Numerical calculations for a spherical restricted geometry confirm these qualitative considerations and show at least an order of magnitude difference between the longitudinal and transverse relaxation times in liquid helium-3.[6,8] For this reason, magnetic relaxation in liquid helium-3 in contact with solids can be represented in a simplified way as follows: At first, because of the very efficient spin diffusion, magnetization is transferred from the bulk liquid to atoms of liquid helium-3, which in a restricted geometry are present in microcracks on the crystal surface where relaxation occurs. Magnetic centers located on solid surfaces evidently strongly influence the relaxation rate.

Such microcracks, which have characteristic sizes 100 Å , on the surface of powders and single crystals of double fluorides have been observed by NMR cryoporometry and atomic-force microscopy.[9,10]

Paramagnetic defect (F) centers appear on the surfaces of these microcracks as a result of large distortions of the crystal lattice. The properties of these centers were studied in Ref. 11 by EPR, conductometry, NMR of ^{19}F, and magnetization measurements. The present work continues the study of both the magnetic properties of the surfaces of double fluorides and the magnetic relaxation of liquid ^3He in contact with a solid substrate — a crystal surface of finely dispersed $LiYF_4$ dielectric powder.

Figure 1 shows the temperature dependence of the longitudinal relaxation rate of nuclei of liquid ^3He in contact with ''dry'' $LiYF_4$ powder. Although the temperature dependence obtained is weak, its slope is obviously opposite to the slope observed in previous investigations of magnetic coupling in experiments on the magnetic relaxation of liquid helium-3 in contact with $LiYF_4$–$LiTmF_4$ single crystals,[6], where the longitudinal relaxation rate was proportional to the magnetization of solid-state magnetic moments and therefore decreased with increasing temperature. To understand the reason for such a radical change in the temperature dependence, we shall write down the expression for the thermal contact of a nuclear spin system of liquid helium-3 and a solid-state substrate on the basis of the relaxation model proposed in Ref. 6:

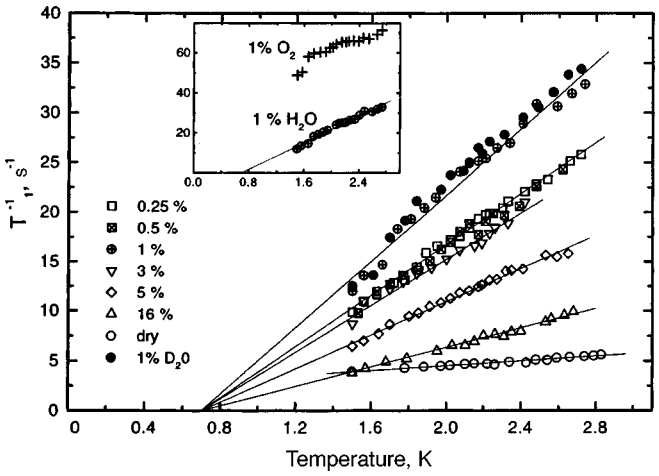

FIG. 1. Temperature dependence of the longitudinal relaxation rate of nuclear spins of liquid helium-3 in pores of ''dry'' micron-size $LiYF_4$ powder (○) and in pores of powder which are filled with distilled water and heavy water for various water molecule concentrations as a percent of the total volume of voids in the sample. Inset: Comparison of the relaxation rates of liquid helium-3 with 1% filling of the voids in the sample with H_2O and O_2.

$$C_{^3\mathrm{He}}\, T_{1,\mathrm{meas}}^{-1} = C_{^3\mathrm{He,bulk}}\, T_{1,\mathrm{diff}}^{-1} + C_{^3\mathrm{He,restr}}\, T_{1,\mathrm{restr}}^{-1}, \tag{1}$$

where

$$C_{^3\mathrm{He}} = C_{^3\mathrm{He,bulk}} + C_{^3\mathrm{He,restr}} \tag{2}$$

is the total magnetic specific heat of nuclear spins of liquid ^{3}He, consisting of two terms referring to, respectively, bulk helium-3 atoms and atoms located in microcracks on the crystal surface (restr). The relaxation time $T_{1,\mathrm{meas}}$ is the measured value, $T_{1,\mathrm{diff}}$ is the characteristic transfer time of the longitudinal magnetization of the nuclear spins of liquid helium-3 from atoms of the bulk liquid to atoms present in the restricted geometry in microcracks on a crystal surface, and $T_{1,\mathrm{restr}}$ is simply the relaxation time of the nuclear magnetizatio n of atoms of liquid ^{3}He in these microcracks. This time can be determined by several mechanisms:

a) direct transfer of magnetization to magnetic moments of the solid-state substrate which have close Larmor frequencies (see, for example, Ref. 2); this mechanism is most efficient when the frequencies are identical (see, for example, Refs. 5 and 12);

b) relaxation of longitudinal magnetization in strongly fluctuating local magnetic fields produced by paramagnetic defect centers on the surfaces of microcracks;

c) relaxation as a result of fluctuations of local fields in the presence of quantum exchange of helium-3 atoms on a solid surface;[13] it is obvious that at temperatures above 1 K this mechanism is inefficient because the number of adsorbed helium-3 atoms is small; and,

d) relaxation in a restricted geometry because of large changes in the spectral characteristics of diffusive motion;[6] our calculations show that this mechanism should make a temperature-independent contribution (if one neglects the temperature dependence of the diffusion coefficient) to the measured relaxation rate.

It follows from Eq. (1) that in our experiments with single crystals[6] the bottleneck of the process is the relaxation of magnetization at the surface because of the small relative fraction of helium-3 atoms in microcracks. It can be concluded from the character of the temperature and field dependences that the dominant relaxation mechanism is the second one mentioned above. Indeed, the increase in magnetization of the paramagnetic defect centers under the influence of temperature or magnetic field leads to an increase in the amplitude of the fluctuating magnetic fields, which accelerates the relaxation process.

In the present experiments with finely dispersed powders the relative fraction of helium-3 atoms in microcracks is high because of the extended crystal surface of micron-size power particles. However, because of the high local magnetic fields in microcracks, the Larmor frequencies of the nuclear spins of the atoms of liquid helium-3 in the microcracks differ quite substantially from the Larmor frequency of the nuclear spins of bulk liquid ^{3}He. It is obvious that in such a situation the bottleneck in relaxation will be the transfer of magnetization from the bulk liquid to the nuclear spins of ^{3}He in the microcracks. For this reason, the increase in magnetization of the paramagnetic defect centers as a result of a decrease in temperature will increase even more the mismatch of the Larmor frequencies and, in consequence, slow down the relaxation of the longitudinal magnetization. In this case, the quite large temperature-independent contribution to the relaxation rate is governed by the relaxation mechanism in the restricted geometry.

Summarizing, we note that the present experiments have confirmed our conjecture[6] that the efficiency of the magnetic relaxation of liquid helium-3 in contact with a solid-state substrate is determined by the competition between two processes: the acceleration of relaxation in nonuniform magnetic fields and the exchange of magnetization between the atoms of liquid helium-3.

To study further the degree to which paramagnetic defect centers on a crystal surface influence the magnetic relaxation of the nuclei of liquid helium-3, we performed experiments to measure the temperature dependence of T_1 for ^{3}He nuclei with various degrees of filling of microcracks on a crystal surface by molecules of distilled water. Finely dispersed $LiYF_4$ powder was placed in a Pyrex glass ampoule with a fill factor of 0.5. The ampoule was evacuated for several days and the powder was exposed to saturated water vapor at room temperature for a certain period of time. After being detached from the reservoir with saturated water vapor, the sample reached an equilibrium state in several hours. The degree of filling of microcracks with water was monitored by NMR cryoporometry, described in Refs. 9 and 10. The longitudinal relaxation rate of the nuclear spins of liquid helium-3 at each temperature was determined from 50 values of the amplitude of the free-induction decay signal for various delay times τ between the rf probe pulses ($\pi/2-\tau-\pi/2$). In all the experiments the evolution of the longitudinal magnetization was described well by a single exponential.

The data from these measurements are displayed in Fig. 1 (open symbols). Comparing the dependences obtained and the measurements of the relaxation rate of nuclei of liquid helium-3 in contact with the ''dry'' $LiYF_4$ powder shows that in the case of the dry

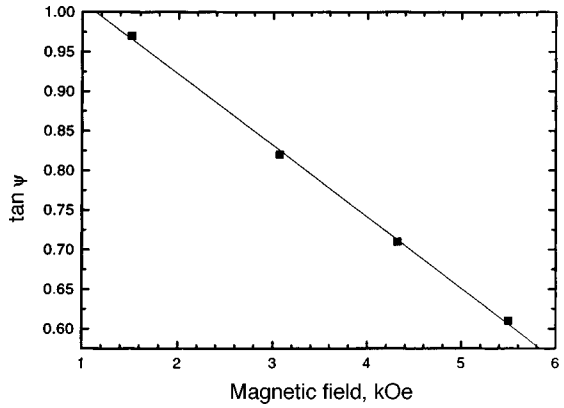

FIG. 2. Field dependence of the slope of $T_1^{-1}(T)$ at $T=1.5$ K with 0.5% filling of the voids in the sample by H_2O molecules.

powder the temperature dependence is quite weak, whereas even a small filling of the microcracks with H_2O molecules increases the magnetic relaxation rate of liquid helium-3 and results in a strong linear Curie–Weiss-type temperature dependence with a characteristic temperature $T_c=0.7$ K. Such behavior of $T_1^{-1}(T)$ indicates that water molecules play a large role both in displacing atoms of liquid helium-3 from microcracks and in the surface magnetism. A very low degree of filling of the microcracks with water influences mainly the decrease in the mismatch of the Larmor frequencies, since water molecules displace the rapidly relaxing atoms of liquid helium-3 from regions with the largest nonuniformities of the local magnetic fields. A further increase of the concentration of water molecules results in a large decrease of the magnetic specific heat of the rapidly relaxing atoms of liquid helium-3 (see Eq. (1)).

The increase in the slope of the temperature dependence of the longitudinal relaxation rate of liquid ^{3}He as the water molecule concentration increases from 0.25% to 1% indicates that the above-mentioned mismatch of the Larmor frequencies decreases, i.e., the spatial fluctuations of the local magnetic fields in the microcracks on the surface decrease. This fact can be explained by the appearance of correlations between the magnetic moments of the defect centers. For this reason, it is reasonable to infer that the paramagnetic defect centers[11] concentrated on the surface form exchange-coupled magnetic pairs or clusters, where the exchange interaction occurs as a result of spin-density transfer via the molecular orbitals of oxygen in the water molecules. This is indicated by the fact that the temperature dependence of the relaxation rate remains unchanged when the protons in the water are replaced by deuterium (Fig. 1, filled symbols). An increase of the temperature decreases the magnetization of such exchange-coupled pairs and, in consequence, increases the relaxation rate of the nuclear magnetization of liquid helium-3. The field dependence of the slope of $T_1^{-1}(T)$ at $T=1.5$ K and 0.5% filling of microcracks with water molecules, as shown in Fig. 2, can serve as an additional argument in support of our picture of the magnetic relaxation of liquid helium-3 in contact with a crystal surface. An increase of the magnetic field and the corresponding suppression of the correlations between the paramagnetic defect centers increase the spatial

nonuniformities of the local magnetic fields in the microcracks and decrease the relaxation rate.

At this stage of the investigations, on account of the lack of detailed information about the wave functions of paramagnetic defect centers, it is impossible to make quantitative estimates of the characteristic temperature for such magnetically coupled pairs and to establish the structure of clusters. However, the experimental value $T_c = 0.7$ K lies within reasonable limits when allowance is made for the two-dimensional character of the arrangement of defect centers and their concentration at the surface.[11]

According to our calculations,[6,8] the mechanism of relaxation in a restricted geometry is most efficient for pores less than 50 Å in size. Therefore it is not surprising that in experiments with water-filled pores the temperature-independent contribution to the magnetic relaxation rate is absent, and extrapolation of all temperature dependences in Fig. 1 gives the same characteristic temperature.

If the above-described magnetic relaxation mechanism due to the formation of exchange-coupled pairs or clusters is correct, then replacing the diamagnetic water molecules by paramagnetic oxygen molecules (which actually means covering the entire surface of the microcracks by a solid-state oxygen film, which could be in a magnetically ordered state) should smooth out the spatial fluctuations of the local magnetic fields and increase the longitudinal relaxation rate. Indeed, such an acceleration by more than a factor of 2 is observed experimentally (inset in Fig. 1).

The experimental data — the temperature, field, and concentration dependences of the longitudinal magnetic relaxation rate of the nuclear spins of liquid helium-3 — can be described by the formula

$$T_1^{-1} = A + \frac{T - T_c}{CB}, \tag{3}$$

where B is the magnetic induction and C is a coefficient that contains information about the magnetic properties of the surface paramagnetic centers and about the magnetic interactions between these centers and the nuclear spins of liquid helium-3. The constant term A describes the contribution of the relaxation mechanism in a restricted geometry.[6]

In conclusion, we note that our investigations make it possible, on the one hand, to determine various channels in the magnetic relaxation of the nuclear spins of liquid helium-3 in contact with a solid. On the other hand, the results obtained show that a quantum liquid — helium-3 — can be used as a probe for investigating the magnetic properties of a solid surface at low and ultralow temperatures. Moreover, the experimentally observed mechanisms make it possible to determine the real possibilities of dynamic polarization of nuclei of liquid helium-3 using paramagnetic centers on a solid surface. In our future work we shall investigate the magnetic relaxation of liquid helium-3 in contact with finely dispersed $LiYF_4$ powder at temperatures below 1 K.

We thank V. A. Atsarkin and V. V. Dmitriev for their interest in this work and for a discussion of the results, and R. Yu. Abdulsabirov and S. L. Korableva for growing the crystals.

This work was supported by the Russian Fund for Fundamental Research under Grant No. 97-02-16470.

[1] R. H. Romer, Phys. Rev. **115**, 1415 (1959); Phys. Rev. **117**, 1183 (1960).
[2] L. J. Friedman, P. J. Millet, and R. C. Richardson, Phys. Rev. Lett. **47**, 1078 (1981).
[3] S. Maegawa, A. Schuhl, M. W. Meisel, and M. Chapellier, Europhys. Lett. **1**, 83 (1986).
[4] F. W. Van Keuls, R. W. Singerman, and R. C. Richardson, Low Temp. Phys. **96**, 103 (1994).
[5] A. V. Egorov, F. L. Aukhadeev, M. S. Tagirov, and M. A. Teplov, JETP Lett. **39**, 584 (1984).
[6] V. V. Naletov, M. S. Tagirov, D. A. Tayurskiĭ, and M. A. Teplov, Zh. Éksp. Teor. Fiz. **108**, 577 (1995) [JETP **81**, 311 (1995)].
[7] A. Abragam, *The Principles of Nuclear Magnetism*, Clarendon Press, Oxford, 1961; IL, Moscow, 1963.
[8] D. A. Tayurskii, in *Extended Abstracts of the XXVIIth Congress AMPERE*, Kazan, 1994, p. 219.
[9] R. Yu. Abdulsabirov, A. A. Bukharaev, A. V. Klochkov *et al.*, http://xxx.lanl gov/cond-mat/9808163 (1998).
[10] R. Yu. Abdulsabirov, A. V. Klochkov, S. L. Korableva *et al.*, Phys. Rev. B, submitted for publication (1998).
[11] A. V. Klochkov, S. P. Kurzin, I. R. Mukhamedshin *et al.*, Appl. Magn. Reson. **14**, 525 (1998).
[12] F. W. Van Keuls, T. J. Gramila, L. J. Friedman, and R. C. Richardson, Physica B **165-166**, 717 (1990).
[13] P. C. Hammel and R. C. Richardson, Phys. Rev. Lett. **52**, 1441 (1984).

Translated by M. E. Alferieff

High-frequency asymptotic behavior of *T*-odd optical effects

V. N. Gridnev
A. F. Ioffe Physicotechnical Institute, Russian Academy of Sciences, 194021 St. Petersburg, Russia

(Submitted 25 February 1999)
Pis'ma Zh. Éksp. Teor. Fiz. **69**, No. 7, 510–513 (10 April 1999)

It is shown that the contribution of low-frequency excitations with characteristic energy $\hbar\omega_l$ to *T*-odd (nonreciprocal) optical effects, including spatial dispersion effects, at optical frequencies $\omega \gg \omega_l$ can be calculated in the zeroth-order approximation with respect to the parameter ω_l/ω. This greatly simplifies their analysis. Some of these effects are found to be frequency independent in the spectral regions where the refractive index $n(\omega) \approx$ const. It is shown that frequency-independent Faraday rotation can be observed in media with zero magnetization, including in media with zero microscopic magnetic moment density.
 [S0021-3640(99)00907-X]

PACS numbers: 78.20.Ls

It is well known that the linear response of a solid, just like any system of charged particles, in the field of an electromagnetic wave with frequency ω is determined primarily by excitations with energies $E_n - E_m = \hbar\omega_{nm} \sim \hbar\omega$, where n and m enumerate the states of the system. Therefore experiments in solids at optical frequencies carry information about excitations with energies ~ 1 eV. Nonetheless, in certain cases it could be desirable to use such experiments to investigate the properties of low-frequency excitations $\omega_{nm} \ll \omega$. This is based on the fact that since $\omega_{nm} \ll \omega$, the dynamics of low-frequency excitations can be excluded from the high-frequency response (i.e., one can set $\omega_{nm} = 0$) in the analysis of a number of optical effects. In these cases the analysis of the high-frequency response is much simpler than the corresponding analysis of the low-frequency susceptibility. For example, in Ref. 1 it was suggested that Faraday rotation measurements in metals with strong electronic correlations ($La_2Sr_xCu_{2-x}O_4$, $YBa_2Cu_3O_{7-\delta}$) at optical frequencies be used to determine the density and sign of the carriers, since the complicated Fermi surface makes it difficult to obtain this information from Hall effect measurements.

In the present letter it is shown that the zeroth approximation in the parameter ω_{nm}/ω can be used not only for the Faraday effect but also for other *T*-odd (nonreciprocal) optical effects, whose existence is due to the nonzero wave vector **k** of light, i.e., spatial dispersion effects. It is also shown that some of these effects are frequency independent in the spectral regions where the refractive index $n(\omega) \approx$ const, and they can be observed in media with nontrivial types of magnetic ordering.

In accordance with the condition $\omega \gg \omega_{nm}$ we will study dispersion optical effects described by the Hermitian part of the permittivity tensor

$$\epsilon_{ik}(\omega,\mathbf{k}) = \frac{4\pi}{\hbar\omega^2 V}\sum_{m,n}\rho_m\left[\frac{J^i_{mn}(\mathbf{k})J^k_{nm}(-\mathbf{k})}{\omega_{nm}-\omega} + \frac{J^k_{mn}(-\mathbf{k})J^i_{nm}(\mathbf{k})}{\omega_{nm}+\omega} - \frac{J^i_{mn}J^k_{nm}+J^k_{mn}J^i_{nm}}{\omega_{nm}}\right], \tag{1}$$

$$\mathbf{J}(\mathbf{k}) = \sum_\alpha \mathbf{J}^\alpha(\mathbf{k}),$$

where $\mathbf{J(k)}$ is the Fourier component of the current operator, $\mathbf{J}^\alpha(\mathbf{k}) = (e_\alpha/2m_\alpha) \times(\boldsymbol{\pi}^\alpha e^{-i\mathbf{k}\cdot\mathbf{r}_\alpha} + e^{-i\mathbf{k}\cdot\mathbf{r}_\alpha}\boldsymbol{\pi}^\alpha)$ is the contribution of the αth particle to the current, $J^k_{nm} = J^k_{nm}(0)$, $\hbar\omega_{mn}$ is the transition energy, and ρ_m is the distribution function. The operator $\boldsymbol{\pi}$, which includes the spin–orbit interaction and the constant vector potential $\mathbf{A}$, has the form $\boldsymbol{\pi} = \mathbf{p} - e\mathbf{A}/c + (2mc^2)^{-1}\mathbf{s}\times\nabla V(\mathbf{r}) - i\mathbf{s}\times\mathbf{k}$, where $\mathbf{s}$ is the spin operator. Ordinarily, the last term in the operator $\boldsymbol{\pi}$ is neglected, but it is important for T-odd optical spatial dispersion effects.

Let us consider the contribution $\Delta\epsilon_{ik}(\omega,\mathbf{k})$ of low-frequency excitations to the permittivity tensor $\epsilon_{ik}(\omega,\mathbf{k})$. To zeroth order in ω_{nm}/ω for $\mathbf{k}\neq 0$ we obtain from Eq. (1)

$$\Delta\epsilon_{ik}(\omega,\mathbf{k}) = \frac{4\pi}{\hbar\omega^3 V}\langle[J^i(-\mathbf{k}),J^k(\mathbf{k})]\rangle. \tag{2}$$

This expression also holds at $\mathbf{k}=0$ for the antisymmetric part of the tensor ϵ_{ik}. Besides the standard Onsager symmetry relations $\Delta\epsilon_{ik}(\omega,\mathbf{k},\eta) = \Delta\epsilon_{ki}(\omega,-\mathbf{k},-\eta)$, expression (2) possesses the additional symmetry $\Delta\epsilon_{ik}(\omega,\mathbf{k},\eta) = -\Delta\epsilon_{ki}(\omega,-\mathbf{k},\eta)$. Here the symbol η denotes here a T-odd quantity that characterizes the state of the medium and is a tensor with respect to spatial transformations. These two symmetry relations are compatible only if $\Delta\epsilon_{ik}(\omega,\mathbf{k},\eta)$ is an odd function of the parameter η, i.e., it describes T-odd optical effects. Hence follows an important and perfectly general result: At optical frequencies it is to T-odd optical effects that the low-frequency excitations make the maximum contribution with respect to the parameter ω_{nm}/ω. It is also important that the approximation $\omega_{nm}/\omega = 0$ greatly simplifies the calculation of $\Delta\epsilon_{ik}(\omega,\mathbf{k})$, reducing it to a calculation of the current commutator. It should be stressed that this result also pertains to spatial dispersion effects, i.e., effects for which $\mathbf{k}\neq 0$.

The commutator in Eq. (2) can be calculated only in a concrete model. In the present letter we consider only the general, model-independent properties of the high-frequency response (2), primarily the frequency dependence of the corresponding optical effects. For this, using expression (2), we write out the first few terms of the expansion of $\Delta\epsilon_{ik}(\omega,\mathbf{k})$ in powers of $\mathbf{k}$ up to terms cubic in $\mathbf{k}$, inclusive, separating explicitly the dependence on $\mathbf{k}$ and ω:

$$\Delta\epsilon_{ik}(\omega,\mathbf{k}) = \frac{1}{\omega^3}e_{iks}g_s + \frac{k}{\omega^3}\gamma_{ikl}m_l + \frac{k^2}{\omega^3}e_{iks}\chi_{sln}m_l m_n + \frac{k^3}{\omega^3}\beta_{iklns}m_l m_n m_s. \tag{3}$$

Here $\mathbf{m}$ is a unit vector parallel to $\mathbf{k}$. On this basis, the vector $\mathbf{g}$ and the tensors $\hat{\gamma}$, $\hat{\chi}$, and $\hat{\beta}$ are T-odd and do not depend on $\mathbf{k}$ and ω. According to the Onsager principle, terms that are even in $\mathbf{k}$ are antisymmetric in i and k, while the odd are symmetric. Therefore

the first terms describe Faraday rotation and the second terms describe nonreciprocal birefringence. We note that in centrosymmetric media $\Delta\epsilon_{ik}(\omega,\mathbf{k})$ is either an even or odd function of $\mathbf{k}$, depending the symmetry of the crystal and the parameter η. We shall assume the parameter η to be macroscopic, since it is only in this case that $\Delta\epsilon_{ik}(\omega,\mathbf{k})$ can be a linear function of η.

Since here we are interested in the propagation of characteristic waves in a medium, to analyze $\Delta\epsilon_{ik}(\omega,\mathbf{k})$ as a function of frequency the wave vector $\mathbf{k}$ must be assumed to be a function of frequency, determined from the solution of the dispersion relation, so that $ck(\omega)/\omega=n(\omega)$, where the latter is the refractive index. The frequency dependence of $\Delta\epsilon_{ik}(\omega,\mathbf{k})$ is simplest in the frequency ranges where $n(\omega)\approx$ const. As a rule, in solids such regions precede the frequencies of atomic (interband) transitions.

We first consider the frequency dependence of the nonreciprocal birefringence. Such birefringence is due to the terms in Eq. (3) that contain odd powers of $\mathbf{k}$. Since we have assumed that $ck(\omega)/\omega=n(\omega)\approx$ const, the contribution of the term linear in $\mathbf{k}$ to birefringence, as is evident from Eq. (3), decreases with increasing frequency as $1/\omega^2$. The contribution of the low-frequency excitations to ordinary ($\mathbf{k}=0$) birefringence, which is a T-even effect, has a similar frequency dependence. In this connection we should note the substantial methodological advantage of measurements of T-odd optical effects. Since the parameter η is macroscopic, in an experiment it is always possible in principle to carry out the transformation $\eta\rightarrow-\eta$ by means of external influences. This greatly increases the accuracy and reliability of the measurements.

The frequency dependence of the contribution cubic in $\mathbf{k}$ to the birefringence is altogether different from a linear dependence: In the region $n(\omega)\approx$ const it is completely frequency independent. Such behavior of an optical effect at frequencies much higher than the resonance frequencies is quite unusual and is a specific feature of optical effects due to spatial dispersion. The decrease with increasing frequency of the term linear in $\mathbf{k}$ and the ω independence of the term cubic in $\mathbf{k}$ should not, of course, be thought to mean that the latter is large in magnitude compared to the former, since such frequency behavior occurs only in comparatively narrow spectral regions. The expansion in $\mathbf{k}$ in Eq. (3) is actually an expansion in the small parameter a/λ, where a is the interatomic distance and λ is the wavelength. For this reason, the effect cubic in $\mathbf{k}$ is quite small in most cases and can be observed only on account of the specific features of the magnetic and electronic structures of the medium.

A much more interesting effect, which likewise exhibits the property of frequency independence, is Faraday rotation of the plane of polarization as a result of the terms in Eq. (3) which are quadratic in $\mathbf{k}$. To obtain the frequency dependence of this effect it is necessary to take into consideration the fact that the rotation angle of the plane of polarization of the light $\theta\propto\omega\epsilon_{xy}$, $(\mathbf{k}\parallel z)$, i.e., it contains an extra frequency factor compared with the corresponding terms in Eq. (3). This gives the well-known behavior of ordinary Faraday rotation ($\mathbf{k}=0$): $\theta\propto 1/\omega^2$. As one can see from Eq. (3), the term quadratic in $\mathbf{k}$ gives a frequency-independent contribution to the Faraday rotation.

In Refs. 2 and 3 frequency-independent Faraday rotation was observed in the transparency region of yttrium iron garnet. It was shown in those works that the observed effect can be explained by the precession of the magnetization in the field of the electromagnetic wave and it can be described phenomenologically by introducing off-diagonal

components of the magnetic permeability tensor at optical frequencies. If the general formula (2) is used as the starting point, this mechanism corresponds to a current operator $\mathbf{J}(\mathbf{k})=(ie/m)\mathbf{s}\times\mathbf{k}$.

My analysis shows that the frequency-independent Faraday rotation is a quite general property of media with macroscopically broken *T*-invariance. Thus, aside from media with spin ferromagnetism, it can also be observed in media with spontaneous orbital ferromagnetism, which corresponds to a current operator $\mathbf{J}(\mathbf{k})=(ie/2m)\mathbf{l}\times\mathbf{k}$, where $\mathbf{l}$ is the orbital angular momentum. We note that for spin and purely orbital ferromagnetism, the existence of an effect quadratic in $\mathbf{k}$ does not require the participation of a spin–orbit interaction, while the contribution of the term with $\mathbf{k}=0$ to rotation in media with spontaneous ferromagnetism is nonzero only if the spin–orbit interaction is taken into account.

More interesting is the possibility of this effect occurring in media with a zero macroscopic magnetic moment density. It is easy to obtain the symmetry-imposed necessary condition for this. For this we note that the rotation angle θ of the plane of polarization for a wave propagating in the direction $\mathbf{m}$ has the dependence $\theta\propto\omega\mathbf{G}\cdot\mathbf{m}$ (Ref. 4), where $\mathbf{G}$ is the gyration vector, dual to the antisymmetric part $\epsilon^{-1}_{[ik]}(\omega,\mathbf{k})$ of the inverse permittivity tensor. Since the expansion of the tensor $\epsilon^{-1}_{ik}(\omega,\mathbf{k})$ in powers of $\mathbf{k}$ is of the same form as Eq. (3), we obtain for the rotation angle associated with the term quadratic in $\mathbf{k}$

$$\theta\propto(k(\omega)/\omega)^2\beta_{ikl}m_i m_k m_l, \tag{4}$$

where β_{ikl} is a *T*-odd pseudotensor, analogous to the tensor α_{ikl} in Eq. (3). Since according to Eq. (4) only the completely symmetric part of the tensor β_{ikl} contributes to rotation, it can be concluded that frequency-independent Faraday rotation is possible in media whose symmetry admits the existence of such a tensor.

Aside from the ferromagnets mentioned above, certain antiferromagnetic magnetic-symmetry classes also admit a tensor with such properties. Thus, in all cubic magnetic-symmetry classes, where the piezomagnetic effect is allowed, for example, in the magnetic class T, the tensor β_{ikl} is completely symmetric and has one independent component β_{xyz}. The Faraday effect should exhibit strong anisotropy in such media.

Let us conclude by calling attention to another, much more complicated, type of magnetic ordering for which frequency-independent Faraday rotation is possible. From the standpoint of symmetry alone the nonzero tensor β_{ikl} in Eq. (4) can exist in magnetic structures whose order parameter is related not with the average microscopic spin density $\langle\mathbf{S}(\mathbf{r})\rangle$, but rather with the three-point spin-density correlation function $\langle S_i(\mathbf{r}_1)S_k(\mathbf{r}_2)S_l(\mathbf{r}_3)\rangle$.[5,6] Here $\langle\mathbf{S}(\mathbf{r})\rangle$ can be zero (in the exchange approximation[5]). If such a correlation function contains a part that is symmetric in the indices *i*, *k*, and *l*, frequency-independent Faraday rotation is also possible in such a medium. Note, however, that the single-time current commutator in relation (2) is not expressed directly in terms of the correlation functions of the spin density, so that the question of the actual existence and magnitude of this effect can be solved only on the basis of a model analysis.

This work is supported by the Russian Fund for Fundamental Research and the program ''Fundamental Spectroscopy.''

[1] B. S. Shastry, B. I. Shraiman, and R. R. P. Singh, Phys. Rev. Lett. **70**, 2004 (1993).
[2] G. S. Krinchik and M. V. Chetkin, Zh. Éksp. Teor. Fiz. **36**, 1924 (1959) [Sov. Phys. JETP **9**, 1368 (1959)].
[3] G. S. Krinchik and M. V. Chetkin, Zh. Éksp. Teor. Fiz. **41**, 673 (1961) [Sov. Phys. JETP **14**, 485 (1962)].
[4] L. D. Landau and E. M. Lifshitz, *Electrodynamics of Continuous Media*, 2nd ed., rev. and enl., by E. M. Lifshitz and L. P. Pitaevskii, Pergamon Press, Oxford, 1984 [cited Russ. edition, Nauka, Moscow, 1992].
[5] V. I. Marchenko, JETP Lett. **48**, 427 (1988).
[6] V. Barzykin and L. P. Gor'kov, Phys. Rev. Lett. **70**, 2479 (1993).

Translated by M. E. Alferieff

Manifestation of magnetically induced spatial dispersion in the cubic semiconductors ZnTe, CdTe, and GaAs

B. B. Krichevtsov,* R. V. Pisarev, and A. A. Rzhevskiĭ
A. F. Ioffe Physicotechnical Institute, Russian Academy of Sciences, 194021 St. Petersburg, Russia

H.-J. Weber†
Department of Physics, Dortmund University, 44221 Dortmund, Germany

(Submitted 26 February 1999)
Pis'ma Zh. Éksp. Teor. Fiz. **69**, No. 7, 514–519 (10 April 1999)

Nonreciprocal birefringence due to magnetically induced spatial dispersion was observed in the T_d-class cubic semiconductors ZnTe, CdTe, and GaAs near the fundamental absorption edge. The dispersion of the parameters A and g, describing the contributions from terms of the type $B_i k_j$ to the diagonal and off-diagonal components of the permittivity tensor $\epsilon_{ij}(\omega,\mathbf{B},\mathbf{k})$, is determined for ZnTe and CdTe. Analysis of the dispersion and anisotropy of the nonreciprocal birefringence shows that in ZnTe, CdTe, and GaAs, in contrast to magnetic semiconductors of the type $Cd_{1-x}Mn_xTe$, it is due excitonic mechanisms. © *1999 American Institute of Physics.* [S0021-3640(99)01007-5]

PACS numbers: 78.20.Fm, 78.20.Ls, 71.35.Gg

Optical phenomena due to magnetically induced spatial dispersion, which are described by terms of the type $\gamma_{ijkl}B_k k_l$ in the expansion of the permittivity tensor $\epsilon_{ij}(\omega,\mathbf{B},\mathbf{k})$, where $\mathbf{k}$ is the wave vector of the light, can be observed in the presence of an external magnetic field $\mathbf{B}$ in crystals without a center of inversion.[1–3] A striking manifestation of magnetically induced spatial dispersion in the transparency region is nonreciprocal birefringence, linear in the magnetic field $\mathbf{B}$ and odd in the wave vector $\mathbf{k}$ of the light. Nonreciprocal birefringence in semiconductors is of interest for several reasons. In contrast to reciprocal birefringence, which is linear in the magnetic field and is allowed only in magnetically ordered crystals,[4] nonreciprocal birefringence can exist in dia- or paramagnets. It is sensitive to the crystal structure and can be observed only in noncentrosymmetric crystals, which fundamentally distinguishes it from the Faraday magnetooptic effect or the Voigt effect, which can be observed in all media. The magnitude of the nonreciprocal birefringence depends on the orientation of the vectors $\mathbf{B}$ and $\mathbf{k}$ relative to the crystal axes and, even in the case of cubic symmetry T_d, it is determined by two independent parameters A and g of the rank-4 axisymmetric tensor γ_{ijkl} which describe, respectively, the contributions of terms of the type $B_k k_l$ in the diagonal and off-diagonal components of the tensor ϵ_{ij}. This opens up new possibilities for studying the anisotropy of the electronic spectrum of cubic noncentrosymmetric crystals. We note that the Faraday effect, the optical activity, and the linear electrooptic effect in class-T_d

cubic crystals are described by rank-3 tensors with only one independent parameter. Nonreciprocal birefringence in semiconductors is directly related with the presence of contributions to the effective Hamiltonian of the electrons, holes, or excitons that are linear in the quasimomentum **q** or bilinear in **q** and **B**. This makes it possible, in principle, to estimate the corresponding parameters of the Hamiltonian, if it is known which optical transitions, interband or excitonic, are responsible for the nonreciprocal birefringence.

Up to now optical phenomena associated with the manifestation of magnetically induced spatial dispersion in semiconductors have been observed in CdSe and CdS (class C_{6v})[5] and GaAs (class T_d)[6] at low temperatures near excitonic transitions. These works investigated the change induced in the intensity of light transmitted through a crystal between crossed polarizers by a transverse magnetic field $\mathbf{k}\perp\mathbf{B}$. Recently, nonreciprocal birefringence was directly observed in the magnetic semiconductors $Cd_{1-x}Mn_xTe$ (class T_d) by a polarimetric method, which made it possible to prove that the effect is odd in **B** and **k** and to determine the parameters A and g.[7,8] Analysis of the concentration dependence and dispersion of the parameters A and g led to the conclusion that nonreciprocal birefringence in magnetic semiconductors is due to the presence of manganese ions and is due to interband optical transitions. The values of the parameters A and g in cubic semiconductors with no magnetic ions have not been determined, and only theoretical estimates are available for their ratio.[6,9] In the present letter we report the observation of a nonreciprocal birefringence in the class-T_d cubic noncentrosymmetric crystals ZnTe and CdTe near the fundamental absorption edge, we investigate the angular and spectral dependences of the nonreciprocal birefringence and determine the parameters A and g and their dispersion, and we compare the results with the magnetic semiconductors $Cd_{1-x}Mn_xTe$ and with theoretical estimates.

Nonreciprocal birefringence was investigated by measuring the rotation α, linear in the magnetic field **B**, of the plane of polarization of light transmitted through a crystal, placed in the gap of an electromagnet, and a quarter-wave plate.[7,8] To study the azimuthal dependence of the birefringence, the crystal was rotated around an axis oriented parallel to the vector **k**. The direction of the magnetic field **B** was set strictly perpendicular to the vector **k** ($\mathbf{k}\perp\mathbf{B}$), since a Faraday effect linear in the magnetic field does not appear in such a geometry. Two combinations of the relative orientations of the polarization **E** of the incident light, the magnetic field **B**, and the principal direction **O** of the quarter-wave plate were used: 1) $\mathbf{E}\parallel\mathbf{B}\parallel\mathbf{O}$ ($\mathbf{E}\parallel\mathbf{B}$ geometry) and 2) $\mathbf{E}\parallel\mathbf{O}$ and with a 45° angle between **E** and **B** (**E**45**B** geometry). The quantity α is determined by the orientation of the principal directions and the ellipticity of the cross section of the indicatrix, which depend on the azimuth θ of the crystal relative to the magnetic field.[7,8] For $\mathbf{k}\parallel[110]$ the angular dependences $\alpha(\theta)$ in the $\mathbf{E}\parallel\mathbf{B}$ (**E**45**B**) geometries can be described by the combination of harmonics $a_1\cos\theta+a_2\cos3\theta$ ($b_1\sin\theta+b_2\sin3\theta$), where $a_{1,2}$ ($b_{1,2}$) are parameters that depend on A and g. Given the experimental dependences $\alpha(\theta)$ and the refractive index, one can determine the parameters A and g. For $\mathbf{k}\parallel[111]$ the functions $\alpha(\theta)$ are described by third-order harmonics. In this geometry the parameter combination $A+2g$ is determined.

A dye laser in the wavelength range 570–610 nm, a titanium–sapphire laser in the range 850–1000 nm, and a helium–neon laser emitting at 633 nm and 1150 mm were used as light sources. The sensitivity of the measurements of the rotations of the polar-

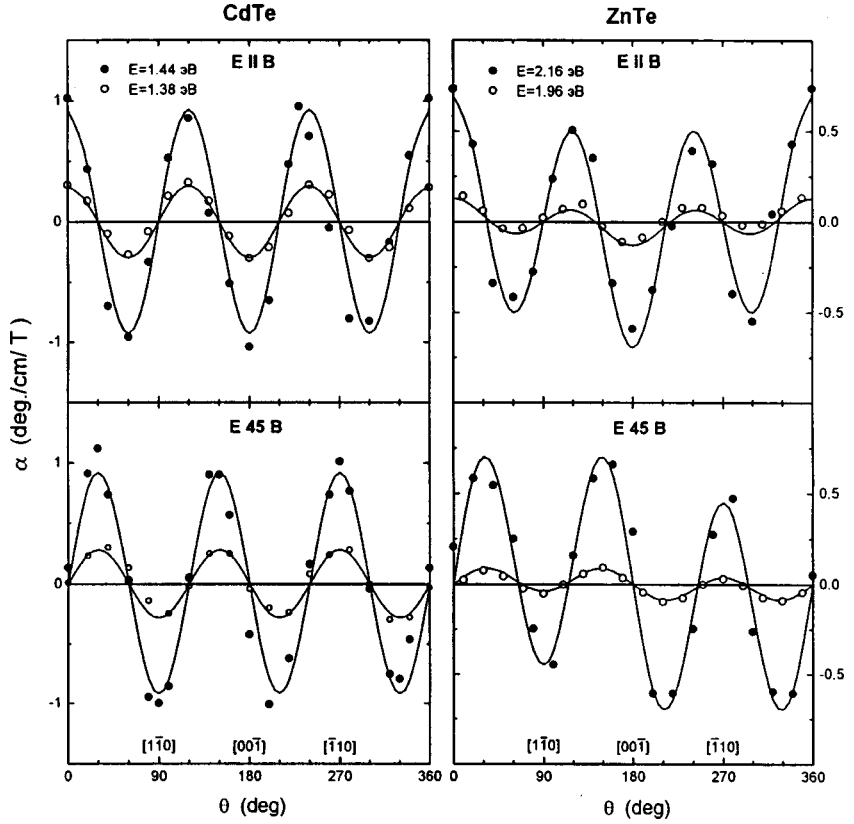

FIG. 1. Angular dependences $\alpha(\theta)$ in ZnTe and CdTe in a (110) type plane ($\theta=0$ corresponds to **B** parallel to a [001] type axis). Solid lines — computational results obtained with adjustable parameters A and g.

ization plane was $\Delta\alpha\sim 10''$. To eliminate any possible influence of photorefraction, the radiation power was limited by means of filters. ZnTe and CdTe single crystals in a (110) type plane and GaAs single crystals in a (111) type plane were investigated. The crystals were $\sim(0.5-1)$ mm thick. The band gap E_g and the spectral dependences of the refractive index n from Refs. 10–12 were used in the calculations. The measurements were performed at $T=294$ K.

Figure 1 displays the angular dependences $\alpha(\theta)/B$, measured at two wavelengths in the geometries $\mathbf{E}\|\mathbf{B}$ and **E**45**B,** in ZnTe and CdTe in a plane of the (110) type. In accordance with the theory, the experimental dependences $\alpha(\theta)$ can be described by harmonics of first and third orders. Both harmonics are observed in ZnTe, and the third-order harmonic $\cos 3\theta$ ($\sin 3\theta$) predominates in CdTe. In GaAs in a (111) type plane, the experimental dependences $\alpha(\theta)$ can be described by harmonics of third order. The nonreciprocal birefringence increases as the fundamental absorption edge is approached. Figure 2a displays α versus the difference E_g-E, where E is the photon energy. The dependences obtained in the geometry $\mathbf{E}\|\mathbf{B}$ at $\theta=0$ ($\mathbf{B}\|[001]$, $\mathbf{k}\|[110]$) are presented for ZnTe and CdTe. In this case $\alpha=\pi gBk/ln$, i.e., it is determined only by the parameter g (l is the sample thickness). For GaAs the dependences in the geometry $\mathbf{E}\|\mathbf{B}$ with

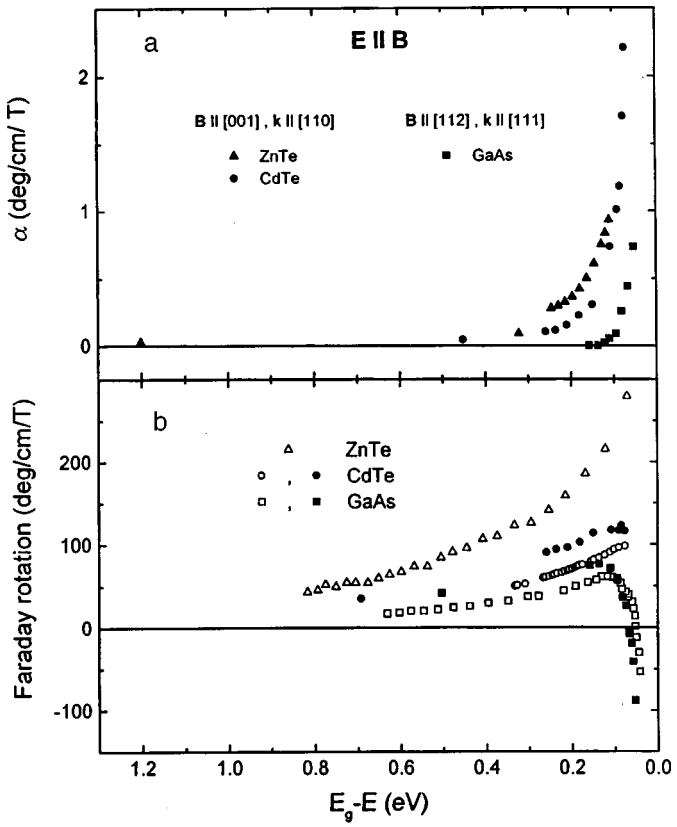

FIG. 2. $\alpha(E_g-E)$ in ZnTe and CdTe with $\mathbf{B}\|[001]$ and GaAs with $\mathbf{k}\|[111]$ and $\mathbf{B}\|[110]$ in the $\mathbf{E}\|\mathbf{B}$ geometry. The bottom panel displays the spectral dependences of the Faraday effect from the present study (filled circles and squares) and from Refs. 13–15 (open circles, triangles, and squares).

$\mathbf{B}\|[112]$ and $\mathbf{k}\|[111]$ are presented. In this case $\alpha=\pi(A+2g)Bk/\sqrt{6}ln$. Far from the edge the the nonreciprocal birefringence is small and is essentially absent for $E_g-E>0.2$ eV. As the band edge is approached, $E\to E_g$, the nonreciprocal birefringence increases sharply, and at $E_g-E\simeq 0.1$ eV it is characterized by a value ~ 2 deg/cm·T. Figure 3 shows the parameters A and g in ZnTe and CdTe as a function of E_g-E. These curves were calculated from the angular and spectral dependences $\alpha(\theta,\lambda)$. The error in determining the parameters is $\sim 15\%$. In both crystals the parameter g increases as $E\to E_g$, and its dispersion is described by the power law $(E_g-E)^{-\tau}$, where $\tau=2.0\pm 0.3$. In ZnTe we have $A\ll g$ in the experimental spectral range. In CdTe the parameter A is approximately 1.5 times smaller than g.

Near the band edge the nonreciprocal birefringence in semiconductors, like other manifestations of magnetically induced spatial dispersion, could be due to interband or excitonic optical transitions. In the case of interband transitions from the valence band Γ_8 into the conduction band Γ_6, a dependence $A\sim(E_g-E)^{-0.5}$ should be expected.[7,8] The contribution of interband transitions to the Faraday effect linear in the magnetic field is likewise described[16] by a dependence $\sim(E_g-E)^{-0.5}$, while the contribution to the

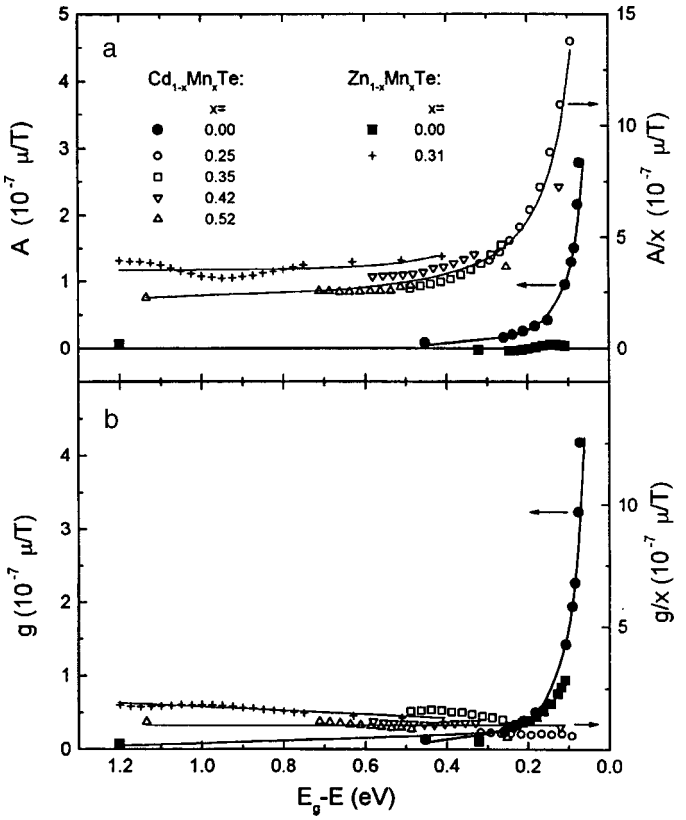

FIG. 3. A and g in ZnTe and CdTe versus $E_g - E$. Solid lines — calculation using the formula $g = t(E_g - E)^{-\tau}$, where t and τ are adjustable parameters.

quadratic Voigt effect is described[17] by the dependence $\sim(E_g - E)^{-1.5}$. Thus, for the interband mechanism the spectral dependences of the nonreciprocal birefringence and the Faraday effect should be similar near the band edge.

The excitonic mechanisms of nonreciprocal birefringence in class-T_d semiconductors have been examined in Ref. 9 for the case of a $1s$ exciton. Including in the effective excitonic Hamiltonian terms linear in **q**,

$$H(\mathbf{q}) = C[q_x\{J_x(J_y^2 - J_z^2)\} + \text{ c.p.}]I_e\,, \tag{1}$$

and linear in **B**,

$$H(\mathbf{B}) = g_e\mu_B \mathbf{s}\cdot\mathbf{B} I_h - 2\mu_B[k\mathbf{J}\cdot\mathbf{B} + q(B_x J_x^3 + \text{c.p.})]I_e \tag{2}$$

(**s** is the electron spin operator; all other notation corresponds to Ref. 9), leads for $E_g - E > 0.1$ eV to dispersion of the parameters A and g: $A = g \sim (E_g - E)^{-1}$ (Ref. 6). When terms bilinear in **q** and **B** are included in the Hamiltonian,

$$H(\mathbf{q},\mathbf{B}) = [B_1([\mathbf{B}\times\mathbf{q}]_x\{J_y J_z\} + \text{c.p.}) + B_2(B_x q_x(J_y^2 - J_z^2) + \text{c.p.})]I_e \tag{3}$$

an increase in the nonreciprocal birefringence $\sim(E_g-E)^{-2}$ is predicted as the edge is approached. The ratio of A and g is this case is determined by the Luttinger parameters, and $A/g\sim(0.1–0.15)$ for ZnTe, CdTe, and GaAs crystals.[9]

The dependence on E_g-E of the rotation α in ZnTe, CdTe, and GaAs (Fig. 2) and of the parameters A and g in ZnTe and CdTe (Fig. 3) show that the nonreciprocal birefringence in the crystals investigated is not due to the interband mechanism and must therefore be attributed to excitonic transitions. This is indicated by the smallness of the effect at a relatively small distance from the band edge ($E_g-E>0.2$ eV), the sharp increase $\sim(E_g-E)^{-2}$ of the effect as the edge is approached, and also a ratio of the parameters A and g that is uncharacteristic of the interband mechanism ($g\gg A$ and ZnTe and $g>A$ in CdTe). The dispersion of the nonreciprocal birefringence in the experimental crystals is substantially different from that of the Faraday effect. The Faraday effect in ZnTe, CdTe, and GaAs is characterized by a relatively large magnitude far from the absorption edge and increases weakly as $E\rightarrow E_g$ (Fig. 2).

The ratio of the parameters A and g and their frequency behavior in ZnTe and CdTe nonetheless is not completely satisfactorily described by the expressions obtained taking into account the contributions in the excitonic Hamiltonian which are linear and bilinear in $\mathbf{q}$ and $\mathbf{B}$.[6,9] In ZnTe $g\gg A$, which does not agree with the estimates obtained in Refs. 6 and 9. In CdTe $g\simeq 1.5A$ (Fig. 3), which approximately corresponds to the mechanism of the contributions linear in $\mathbf{q}$ and $\mathbf{B}$, but the dispersion of A and g is stronger, $\sim(E_g-E)^{-2}$, than that predicted by the model, $\sim(E_g-E)^{-1}$. In our opinion this discrepancy is due to the fact that terms which are linear and bilinear in $\mathbf{q}$ and $\mathbf{B}$ must be taken into account simultaneously in the excitonic Hamiltonian. In this case g can be greater than A if the contributions of the linear and bilinear terms have different signs. Another possible reason for the discrepancy between the experimental and theoretical dependences of the parameters A and g could be the inadequacy of taking account of only the $1s$ excitonic states, since contributions of higher excitonic states, including states of unbound excitons, could contribute to the nonreciprocal birefringence.

The dispersion of the parameter A and that of the Faraday effect are close in the magnetic semiconductors $Cd_{1-x}Mn_xTe$. This attests to an interband mechanism. The stronger dispersion of the nonreciprocal birefringence and the Faraday effect in magnetic semiconductors, $\sim(E_g-E)^{-1.5}$, than predicted by the interband transition model, $\sim(E_g-E)^{-0.5}$, can be explained by the dependence of the parameters of the exchange interaction of electrons and holes with the $3d$ electrons of Mn^{2+} ions on the wave vector $\mathbf{q}$.[7,13] Taking account of this dependence also permits explaining the strong dispersion of the Voigt effect $\sim(E_g-E)^{-3.5}$ in $Cd_{1-x}Mn_xTe$.[18]

The strong differences in the spectral behavior of the parameters A and g (Fig. 3) likewise attest to different mechanisms of magnetically induced spatially dispersion in pure and Mn-containing semiconductors. The parameter g in magnetic semiconductors is virtually dispersionless, while in pure semiconductors it is observed to increase sharply as E_g is approached. In the magnetic semiconductors $Zn_{1-x}Mn_xTe$ and $Cd_{1-x}Mn_xTe$ the parameter A is much greater than g, while in ZnTe and CdTe the parameter g is greater than A.

In summary, our investigation has shown that nonreciprocal birefringence due to magnetically induced spatial dispersion is observed near the fundamental absorption edge

in the cubic noncentrosymmetric semiconductors ZnTe, CdTe, and GaAs. Analysis of the dispersion and anisotropy of the nonreciprocal birefringence and comparison with the spectral dependences of the Faraday effect in pure and Mn-containing semiconductors led to the conclusion that in pure semiconductors, in contrast to magnetic semiconductors, the nonreciprocal birefringence is due not to interband but rather to excitonic mechanisms. Further elaboration of the theory is required in order to give an adequate description of the anisotropy and dispersion of the nonreciprocal birefringence.

This work was supported by the Russian Fund for Fundamental Research, the program ''Fundamental Spectroscopy,'' and DFG.

We thank D. Froehlich, A. A. Berezhnyĭ, and Yu. V. Zhilyaev for providing the crystals and N. F. Kartenko for performing the x-ray crystallographic investigations.

*e-mail: krichev@star.ioffe.rssi.ru
†e-mail: weberhj@fkp.physik.uni-dortmund.de

[1] D. L. Portigal and E. Burstein, J. Phys. Chem. Solids **32**, 603 (1971).
[2] V. M. Agranovich and V. L. Ginzburg, *Crystal Optics with Spatial Dispersion, and Excitons*, Springer-Verlag, New York, 1984, 2nd corrected and updated edition [Russian original, Nauka, Moscow, 1979].
[3] P. Etchegoin, A. Fainstein, P. Santos *et al.*, Solid State Commun. **92**, 505 (1994).
[4] V. V. Eremenko, N. F. Kharchenko, Yu. G. Litvinenko, and V. N. Naumenko, *Magneto-Optics and Spectroscopy of Antiferromagnets*, Naukova dumka, Kiev, 1989.
[5] E. L. Ivchenko, V. P. Kochereshko, G. V. Mikhaĭlov, and I. N. Ural'tsev, JETP Lett. **37** 164 (1983); Phys. Status Solidi B **121**, 221 (1984).
[6] O. V. Gogolin, V. A. Tsvetkov, and E. G. Tsitsishvili, Zh. Éksp. Teor. Fiz. **87**, 1038 (1984) [Sov. Phys. JETP **60**, 593 (1984)].
[7] B. B. Krichevtsov, R. V. Pisarev, A. A. Rzhevsky *et al.*, Phys. Rev. B **57**, 14611 (1997).
[8] B. B. Krichevtsov, R. V. Pisarev, A. A. Rzhevskiĭ *et al.*, Zh. Éksp. Teor. Fiz. **114**, 1018 (1998) [JETP **87**, 553 (1998)].
[9] E. G. Tsitsishvili, Fiz. Tekh. Poluprovodn. **20**, 650 (1986) [Sov. Phys. Semicond. **20**, 412 (1986)].
[10] J. K. Furdyna, J. Appl. Phys. **64**, R29 (1988).
[11] D. T. F. Marple, J. Appl. Phys. **35**, 539 (1964).
[12] J. S. Blakemore, J. Appl. Phys. **53**, R123 (1982).
[13] S. Hugonnard-Bruyère, C. Buss, F. Vouilloz *et al.*, Phys. Rev. B **50**, 2200 (1994).
[14] W. Thielmann and B. Rheinländer, Phys. Status Solidi **14**, K205 (1966).
[15] D. U. Bartholomew, J. K. Furdyna, and A. K. Ramdas, Phys. Rev. B **34**, 6943 (1986).
[16] L. Roth, Phys. Rev. A **133**, 542 (1964).
[17] M. Cardona, Helv. Phys. Acta **34**, 796 (1961).
[18] B. B. Krichevtsov, R. V. Pisarev, A. A. Rzhevskiĭ *et al.*, JETP Lett. **67**, 602 (1998).

Translated by M. E. Alferieff

Electronic contribution to sliding friction in normal and superconducting states

V. L. Popov*

Institute of the Physics of Strength and Materials Science, Siberian Branch of the Russian Academy of Sciences, 634021 Tomsk, Russia

(Submitted 3 March 1999)
Pis'ma Zh. Éksp. Teor. Fiz. **69**, No. 7, 520–523 (10 April 1999)

The electronic contribution to friction between an atomically flat metal surface and a dielectric layer absorbed on the surface is calculated. The friction force decreases abruptly at the transition of the metal to the superconducting state. © *1999 American Institute of Physics.* [S0021-3640(99)01107-X]

PACS numbers: 46.55.+d, 68.35.Wm

In the last few years new experimental and computational possibilities have rapidly increased the understanding of fundamental friction processes.[1,2] Specifically, it has been shown experimentally[3,4] and theoretically[5–8] that in an ''atomically close'' contact between two crystal bodies there is no static friction provided that the periods of the crystal lattices of the bodies in contact are incommensurate. An additional condition is that there must be no ''elastic instabilities'' at the contact of the two bodies, i.e., a unique equilibrium state of the system must correspond to each set of boundary conditions at infinity. If the interaction of the surfaces is sufficiently weak, the condition that the contact be monostable is always satisfied and the static friction vanishes. This situation is characteristic, for example, for solid layers of inert gases adsorbed on gold and silver.[4] However, the absence of static friction has also been confirmed experimentally for a tungsten–silicon contact.[3] The latter example, which is a ''metal–covalent crystal'' tribological contact, shows that zero static friction between crystalline materials with incommensurate lattices can also occur in systems which could be of practical value.

I shall assume in what follows a contact with zero static friction. However, this does not mean that there is no friction at all. Generally speaking, the interaction of surface atoms results in phonon generation and excitation of the electronic subsystem. This is manifested in the presence of a ''viscous'' friction force, which is proportional to the relative velocity of the moving bodies. Even though the phonon[9,10] and electronic[11,12] contributions to this viscous force have been intensively investigated theoretically, their magnitude and ratio are still a subject of debate. Apparently, the most direct method for distinguishing the electronic contribution could be the measurement of the friction force near a superconducting transition. Masurements of the friction force between a layer of lead and a solid layer of N_2 adsorbed on the lead have shown that the friction force exhibits a jump, which cannot be explained in existing theoretical models, at the superconducting transition point.[13] Indeed, the fraction of electrons forming the superconduct-

ing condensate increases continuously from zero at temperatures below T_c. The remaining normal electrons must once again be excited by the adsorbed layer. Therefore the friction stress below T_c should decrease continuously. In the present letter it is shown that the model which I proposed in previous work,[14] describing the electronic contribution to the friction force, gives a simple explanation of this effect.

Let us consider a metal sample in the form of a parallelepiped of thickness d, on one surface of which a crystalline monolayer of a dielectric is adsorbed. Let the (x,z) plane be the friction surface, and let the x axis be oriented in the direction of the relative motion of the metal sample and the adsorbed layer. The spectrum of the electron gas does not satisfy the Landau superfluidity condition. Therefore the electrons will be excited by the moving monolayer and be ''dragged'' by it. If the electron mean free path l_N with respect to normal scattering processes (with conservation of the quasimomentum) is much shorter than the mean free path l_U with respect to processes that violate conservation of quasimomentum (Umklapp processes and scattering by lattice nonuniformities), the electron gas in the crystal is governed by a hydrodynamic equation. For a stationary flow in the geometry described above, this equation has the form

$$\eta\frac{\partial^2 V}{\partial y^2}-\frac{\rho V}{\tau_U}=0. \tag{1}$$

Here $V=V(y)$ is the x component of the hydrodynamic velocity of the electron gas, η is the viscosity of the electron gas, ρ is the mass density of the gas, and τ_U is the characteristic free flight time with respect to processes that violate quasimomentum conservation. The characteristic length

$$l=(\eta\tau_U/\rho)^{1/2} \tag{2}$$

can be formed from the coefficients in Eq. (1). The condition of applicability of Eq. (1) is that the mean free path l_N must be smaller than the dimensions of the body. Since we are assuming that $l_U\gg l_N$, we have $l\approx(l_U l_N)^{1/2}\gg l_N$ (see Ref. 14). Therefore Eq. (1) is also applicable at distances less than the characteristic length l.

There is an important circumstance not taken into account in Eq. (1). The described ''dragging'' of the electron gas and the associated surface current will inevitably give rise to an electric field and a counterflowing ''bulk'' current. In the presence of an electric field Eq. (1) must be modified as follows:

$$\eta\frac{\partial^2 V}{\partial y^2}-\frac{\rho V}{\tau_U}+enE=0, \tag{3}$$

where e is the elementary charge, n is the electron density, and E is the intensity of the electric field. This last quantity is itself determined by the condition that the total current in the sample vanishes.

We shall consider separately the limiting cases of thick ($d\gg l$) and thin ($d\ll l$) metal layers.

I. $d\gg l$. The solution of Eq. (3) that is bounded in the direction into the sample ($y\to\infty$) and satisfies the condition that the total current in the sample is zero,

$$\int_0^d V(y)dy = 0, \tag{4}$$

has the form

$$V(y) = -V_0 \frac{l/d}{1-l/d} + V_0 \frac{1}{1-l/d} \exp(-y/l), \tag{5}$$

where V_0 is the velocity of the adsorbed layer.

Since the only friction mechanism considered here is momentum transfer to the body of the crystal through the electron gas, the friction stress can be determined as the viscous stress in the electron gas at $y=0$:

$$|\sigma_n| = \eta \left| \frac{\partial V}{\partial y} \right|_{y=0} = \eta \frac{V}{l} (1-l/d)^{-1}. \tag{6}$$

Thus the correction due to the return current is of the order of l/d and can be neglected for massive samples (for $d \gg l$).

II. $d \ll l$. The effect of the reverse field turns out to be substantial for thin layers. This case corresponds to the conditions of the experiment of Ref. 13, where lead electrodes 1500 Å thick, deposited on a quartz crystal, were used.

a) *Metal in the normal state.* The solution of Eq. (3) satisfying the boundary conditions $V(0)=V_0$ and $V(d)=0$ and the condition (4) has the form

$$V(y) = V_0(1-4y/d+3(y/d)^2). \tag{7}$$

The friction stress is

$$|\sigma_n| = \eta \left| \frac{\partial V}{\partial y} \right|_{y=0} = \eta \frac{4V_0}{d}. \tag{8}$$

b) *Metal in the superconducting state.* In this case the return current is due to the flow of superconducting electrons at $E \equiv 0$. Correspondingly, the flow of the electron gas in the sample is determined by Eq. (1) with the same boundary conditions as above. Its solution is

$$V(y) = V_0(1-y/d). \tag{9}$$

The friction stress is

$$|\sigma_s| = \eta \left| \frac{\partial V}{\partial y} \right|_{y=0} = \eta \frac{V_0}{d}. \tag{10}$$

Comparing Eqs. (8) and (10) shows that the friction stress due to the conduction electrons changes abruptly at the superconducting transition point, and the friction stress in thin samples ($d \ll l$) decreases by a factor of 4 at the transition of the metal to the superconducting phase.

In the general case of a metal layer of arbitrary thickness the solution of Eq. (3) with the additional equation (4) for a metal in a normal state and Eq. (1) for a metal in the superconducting state gives the following expressions for the friction stress:

$$|\sigma_s| = \frac{\eta V_0}{l} \frac{e^{d/l} + e^{-d/l}}{e^{d/l} - e^{-d/l}} \tag{11}$$

in the superconducting state, and

$$|\sigma_n| = \frac{\eta V_0}{l} \frac{(1 + d/l)e^{-d/l} - (1 - d/l)e^{d/l}}{4 - 2(e^{d/l} + e^{-d/l}) + (d/l)(e^{d/l} - e^{-d/l})} \tag{12}$$

in the normal state. The experimentally observed ratio $\sigma_n/\sigma_s \approx 2$ (Ref. 13) obtains for $d/l \approx 2.3$. Therefore $l \approx 650$ Åis the characteristic perturbation length of the electron gas in lead. Inclusion of the phonon contribution to the friction force does not change this result, since, according to the results of Ref. 14, the phonon contribution to the friction force at the superconducting transition temperature in lead (7.2 K) is much smaller than the electronic contribution.

In summary, we have shown that the physical reason for the jump in the friction force at a superconducting transition is that energy dissipation is due to both a surface current, arising as a result of the electrons being ''dragged'' in the friction surface, and a return current, which arises in order for the sample to remain electrically neutral. In the superconducting state the second of these contributions is ''switched off'' at the transition point, since the return current is transported by the superconducting electrons without dissipation.

I thank the Alexander Humboldt Foundation for financial support.

*Current address: Department of Physics, University of Paderborn, D-33098 Paderborn, Germany.

[1] J. Krim, Sci. Am. (Int. Ed.) **275**, 74 (1996).
[2] B. N. J. Persson and E. Tossatti (Eds.), *Physics of Sliding Friction* (Proceedings of the NATO Adriatico Research Conference on the Physics of Sliding Friction in June 1995), Kluwer Academic Publishers, Dordrecht, 1996.
[3] M. Hirano, K. Shinjo, R. Kaneko, and Yo. Murata, Phys. Rev. Lett. **78** 1448 (1997).
[4] M. O. Robbins and J. Krim, MRS Bull. **23**, 23 (1998).
[5] E. D. Smith, M. O. Robbins, and M. Cieplak, Phys. Rev. B **54**, 8252 (1996).
[6] H. Matsukawa and H. Fukuyama, Phys. Rev. B **49**, 17286 (1994).
[7] T. Gyalog, M. Bammerlin, R. Lüthi *et al.*, Europhys. Lett. **31**, 269 (1995).
[8] T. Gyalog and H. Thomas, Europhys. Lett. **37**, 195 (1997).
[9] M. Cieplak, E. D. Smith, and M. O. Robbins, Science **256**, 1209 (1994).
[10] M. S. Tomassone, J. B. Sokoloff, A. Widom, and J. Krim, Phys. Rev. Lett. **79**, 4798 (1997).
[11] B. N. J. Persson, Phys. Rev. B **44**, 3277 (1991).
[12] J. B. Sokoloff, Phys. Rev. B **52**, 5318 (1995).
[13] A. Dayo, W. Alnasrellah, and J. Krim, Phys. Rev. Lett. **80** 1690 (1998).
[14] V. L. Popov, Tribologie und Schmierungstechnik, No. 2 (1999).

Translated by M. E. Alferieff